EurJIC
European Journal of Inorganic Chemistry

Full Papers
doi.org/10.1002/ejic.202100170

Chemistry Europe
European Chemical Societies Publishing

The Reactivity of Multidentate Schiff Base Ligands Derived from Bi- and Terphenyl Polyamines towards M(II) (M=Ni, Cu, Zn, Cd) and M(III) (M=Co, Y, Lu)

Knut Tormodssønn Hylland,*[a, b] Isabelle Gerz,[a, b] David S. Wragg,[a, b] Sigurd Øien-Ødegaard,[a, b] and Mats Tilset*[a, b]

Multidentate Schiff base ligands derived from a selection of biphenyl- and terphenyl polyamines were synthesized, and their reactivity towards divalent (Ni, Cu, Zn, Cd) and trivalent (Co, Y, Lu) metals was studied by single-crystal X-ray diffraction analysis, NMR spectroscopy, and UV/Vis spectroscopy for the Cu(II) complexes. Large variations in the resulting complexes were observed based on the relative position of the amine substituents in the parent triamines, as well as the electronic properties of the Schiff base ligand itself. Most notably, Schiff base ligands derived from a *m*-terphenyl-2,2′,2″-triamine were found to coordinate in a tetradentate, pentadentate or hexadentate fashion, depending on the size and the valency of the corresponding metal center.

Introduction

Schiff base ligands are popular multidentate ligands in coordination chemistry. Among other things, the popularity arises from the general broad scope of the synthesis of such ligands; a large number of ligands with different denticities can be made from relatively simple precursors.[1] Schiff base complexes of most metals in the periodic table are known,[2] and both Schiff bases and their corresponding metal complexes have found applications within numerous fields, such as catalysis,[3] medicine,[4] supramolecular chemistry[5] and materials science.[6] Of the various Schiff base ligands that are known, tetradentate salen and salen-like ligands are amongst the most studied,[1,3a,7] but ligands with higher denticities are also common.[2,8] Multidentate Schiff base ligands are versatile in the sense that they can stabilize a wide range of coordination geometries and numbers, which makes them suitable ligands for both relatively small metals,[3a,7,9] as well as larger metals.[10] Biphenyl- or terphenyl-2,2′-diamines are attractive starting materials for the synthesis of multidentate Schiff bases, as the 1,4-relation between the amino-groups permits for the formation of a salen-like chelate. Furthermore, the electronic and steric properties of the biphenyl/terphenyl backbone can easily be tuned by standard methods in organic synthesis. Ligands derived from *m*-terphenyls are particularly interesting in coordination chemistry and organometallic chemistry,[11] due to their increased steric bulk compared to the corresponding biphenyls and *p*-terphenyls. In addition, the *m*-terphenyl backbone allows for the installation of three donating moieties in close spatial proximity to each other by functionalization of the positions *ortho* to the C_{Ar}–C_{Ar} bonds (**A**, Figure 1). Although this latter point has been explored to great extent for *m*-terpyridine systems[12] (**B**, Figure 1), relatively few studies have been conducted on tri-*ortho*-substituted *m*-terphenyl ligands.[13]

We recently reported a detailed study on Zn(II) Schiff base complexes derived from biphenyl-2,2′-diamines.[14] Therein, particular focus was devoted to NMR investigations of the metal complexes in solution in the presence or absence of external ligands, such as organic nitrogen-containing bases and Lewis basic solvents (Figure 2a). Several of these complexes were investigated by single-crystal X-ray diffraction as well. In addition to the studies on Zn, Cd complexes of the same ligand systems were investigated.

As a continuation of the work on the Zn complexes in Figure 2a, it was in our interest to investigate Zn complexes with additional Lewis basic groups in the ligand backbone, by

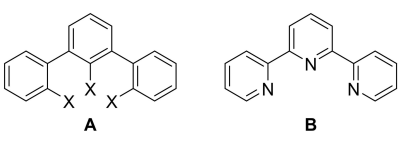

Figure 1. *m*-Terphenyls with donor groups in the positions *ortho* to the C_{Ar}–C_{Ar} bonds (**A**), and *m*-terpyridine (**B**).

[a] Dr. K. T. Hylland, I. Gerz, Dr. D. S. Wragg, Dr. S. Øien-Ødegaard, Prof. Dr. M. Tilset
Department of Chemistry
University of Oslo
P. O. Box 1033 Blindern, 0315 Oslo, Norway
E-mail: k.t.hylland@smn.uio.no
mats.tilset@kjemi.uio.no
http://www.mn.uio.no/kjemi/personer/vit/matst/index.html
[b] Dr. K. T. Hylland, I. Gerz, Dr. D. S. Wragg, Dr. S. Øien-Ødegaard, Prof. Dr. M. Tilset
Centre for Materials Science and Nanotechnology
University of Oslo
P.O. Box 1126 Blindern, 0316 Oslo, Norway

Supporting information for this article is available on the WWW under https://doi.org/10.1002/ejic.202100170

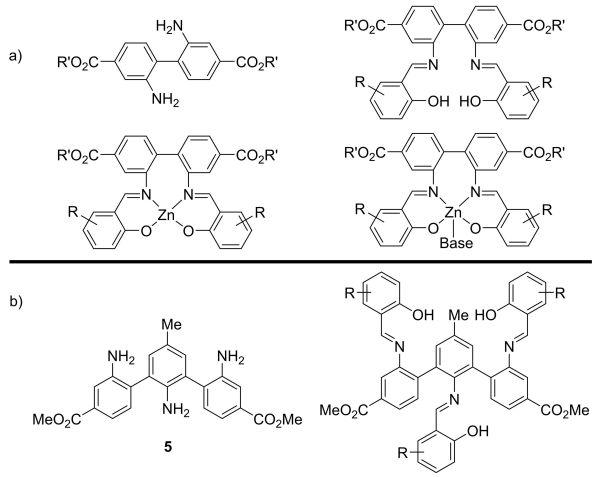

Figure 2. (a) General structure of biphenyl-2,2′-diamines, Schiff base ligands derived from these, and their corresponding Zn complexes that were previously studied by us.[14] (b) *m*-Terphenyl-2,2′,2″-triamine **5** and the general structure of its corresponding Schiff base ligands. The reactivity of these ligands towards different metals will be discussed herein.

employing a *m*-terphenyl-2,2′,2″-triamine rather biphenyl-2,2′-diamines as ligand precursors (Figure 2b). Furthermore, metal complexes with pendant Lewis basic groups in the ligand backbone are useful in catalysis,[15] and as building blocks in supramolecular chemistry.[5c,16] The introduction of an additional salicylaldimine group would further make it possible to obtain potential hexadentate Schiff base ligands, for the coordination of larger metals, such as the rare-earth elements. Herein, we report a study of a series of Schiff base ligands, comprising three salicylaldimine groups in the ligand backbone, and their reactivity towards a selection of metals (Cu(II), Zn(II), Cd(II), Co(III), Y(III) and Lu(III)), showing the flexible nature of these ligands. In addition, we present the synthesis and characterization of Ni(II), Cu(II) and Co(III) analogues of the Zn(II) complexes shown in Figure 2a, in order to further demonstrate the versatility of the biphenyl-2,2′-diamine backbone for the synthesis of metal Schiff base complexes.

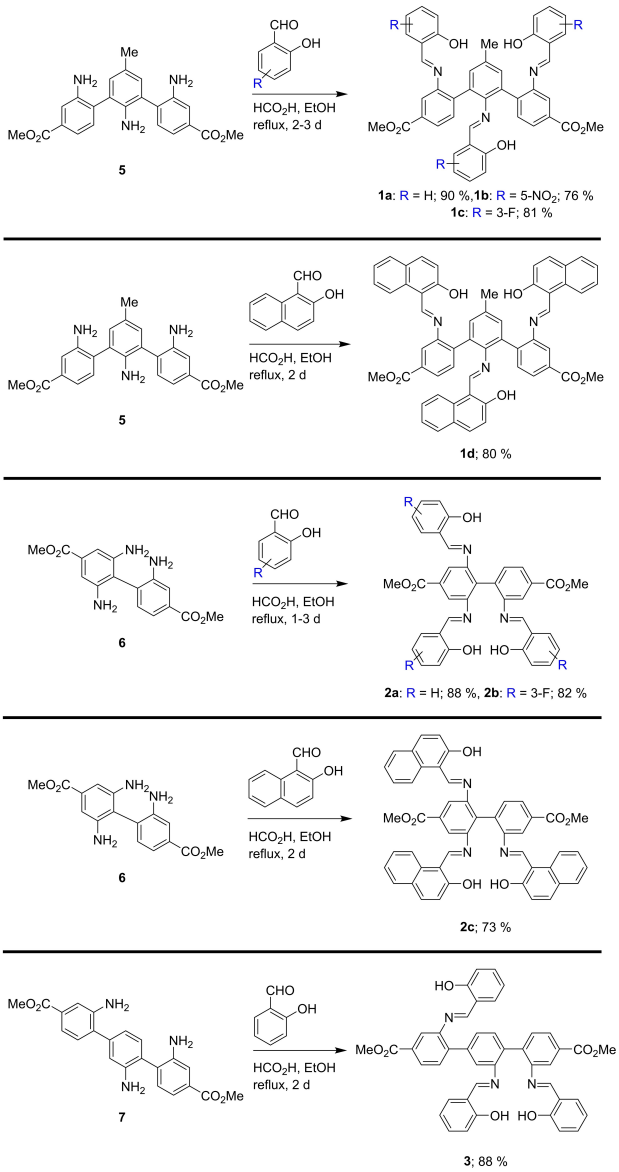

Scheme 1. Synthesis of Schiff base ligands **1a**–**d**, **2a**–**c** and **3** from triamines **5**, **6** and **7**.

Results and Discussion

Synthesis of Schiff base ligands 1a–d, 2a–c and 3

In a recent publication we reported the synthesis of biphenyl- and terphenyl triamines using the Suzuki-Miyaura reaction of bromoanilines and an *ortho*-nitro-substituted arylboronic acid as the key step.[17] Some of these triamines (**5**, **6**, and **7**, Scheme 1) were subjected to typical synthesis conditions for formation of Schiff bases giving access to ligands **1a**–**d**, **2a**–**c** and **3** (Scheme 1).

The ligands were obtained in good yields and were conveniently purified by recrystallization. Because of the relatively large functional groups in the positions *ortho* to the C_{Ar}–C_{Ar} bonds of *m*-terphenyls **1a**–**d**, two rotamers were observed in the NMR spectra of these ligands. The extent of this phenomenon was dependent on the exact substitution pattern of the phenolic rings for each ligand and was most pronounced for **1b** and **1d**. As expected for compounds exhibiting rotamers in their ^{1}H NMR spectra,[18] the ^{1}H NMR resonances of the ligands were solvent- and temperature-dependent (see SI). Although Schiff bases derived from aromatic amines often are quite robust towards hydrolytic degradation in the absence of strong acids or bases,[19] it was found that ligand **1b** would undergo partial hydrolysis in [D_6]DMSO, and the hydrolytic sensitivity of **1b** is a key aspect of its reactivity towards Cu(II), Zn(II) and Cd(II) (*vide infra*). One of the ligands, **1d**, was analyzed by single-crystal X-ray diffraction analysis (Figure 3). The C_{Ar}–C_{Ar} dihedral angles in the ligand were found to be −68.4(2)° and −61.8(2)°, which is comparable to what has been earlier

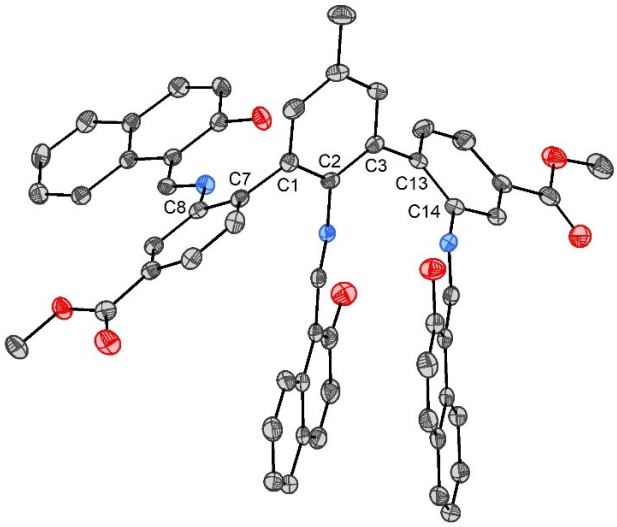

Figure 3. ORTEP plot of **1d** with 50% probability ellipsoids. Hydrogen atoms have been omitted for clarity. Selected angles [°]: C2–C1–C7–C8, −68.4(2), C2–C3–C13–C14, −61.8(2).

reported for sterically encumbered *m*-terphenyls in the literature.[11c,i,17]

Synthesis and NMR studies of Zn complexes 1a-Zn, 1d-Zn, 2a-Zn and 3-Zn

Monometallic Zn(II) complexes of ligands **1a**, **1d**, **2a** and **3** were synthesized by reacting the appropriate ligand with one equivalent of $Zn(OAc)_2 \cdot 2H_2O$ in the presence of an excess of NEt_3 in MeOH or CH_2Cl_2/MeOH (Scheme 2).

The complexes were characterized by NMR spectroscopy, MS, elemental analysis, and single-crystal X-ray diffraction analysis (*vide infra*). From NMR studies of complexes **2a**-**Zn** and **3**-**Zn**, the behavior in solution was largely analogous to what has earlier been reported for Zn complexes of biphenyl- and terphenyl-based tetradentate N_2O_2 ligands.[14,17] No evidence was found for the coordination of the third salicylaldimine group to Zn. For complex **1a**-**Zn**, ^{1}H NMR studies were somewhat less straightforward. In strongly Lewis basic solvents ([D_6]DMSO, [D_7]DMF and [D_5]pyridine), the ^{1}H NMR spectrum of the complex was relatively conventional, although modest broadening of some of the ^{1}H NMR resonances was observed at ambient temperature (*vide infra*). The ^{1}H NMR spectrum of **1a**-**Zn** in $CDCl_3$ revealed the presence of two species, which were observed to interconvert by NOESY experiments (see Figure S127–S129, SI). Whereas the ^{1}H NMR resonances corresponding to the major species underwent changes on gradually increasing the concentration of **1a**-**Zn** in $CDCl_3$, the resonances corresponding to the minor species remained practically constant (Figure 4).

For the major species in the ^{1}H NMR spectrum of **1a**-**Zn**, the resonances became more broadened and were moved to lower ppm values at increased concentrations of **1a**-**Zn**, which is in accordance with the formation of a dimeric (or oligomeric)

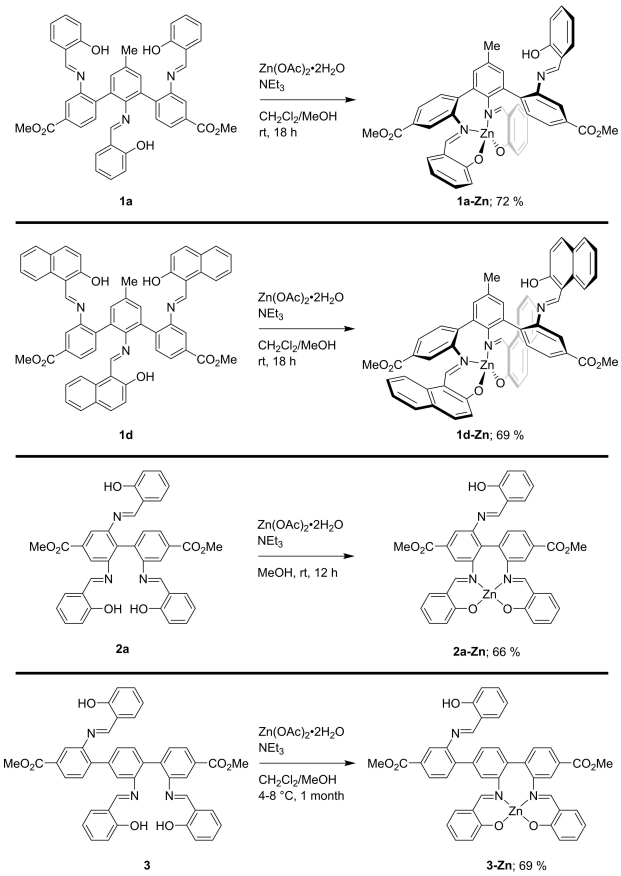

Scheme 2. Synthesis of Zn(II) complexes **1a**-**Zn**, **1d**-**Zn**, **2a**-**Zn** and **3**-**Zn**.

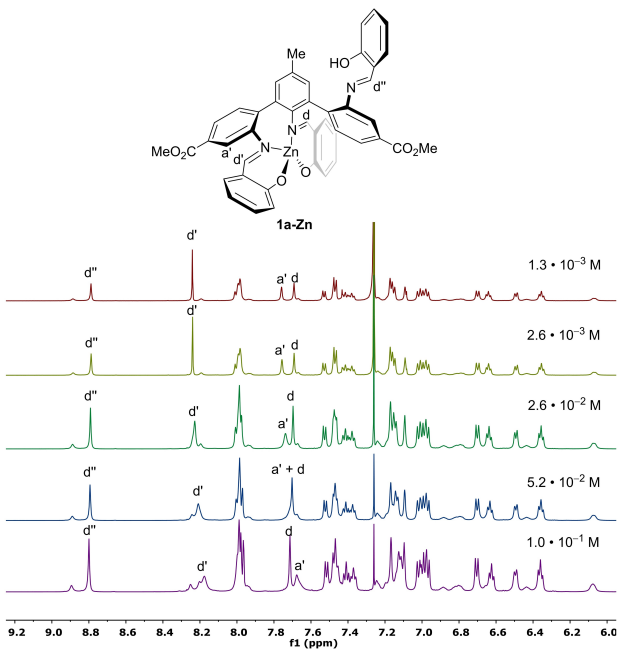

Figure 4. Stacked ^{1}H NMR (600 MHz, $CDCl_3$) spectra of **1a**-**Zn** with different concentrations of the complex. The complex is depicted as a tetracoordinated monomer for simplicity.

species[20] (**1a-Zn**–**D**, Scheme 3). The presence of the additional salicylaldimine group in close proximity to the metal center in **1a-Zn** should facilitate coordination of the imine nitrogen to Zn, resulting in a pentacoordinated monomer (**1a-Zn-5**, Scheme 3). The ^{1}H NMR resonances of this species were unaffected by changes in concentration of the complex, as the coordination of the pendant salicylaldimine group is intramolecular, and not intermolecular like the dimerization process. Hence, **1a-Zn-5** is suggested to be the minor species at any concentration of the complex in $CDCl_3$.

The formation of an N_3O_2-ligated pentacoordinated monomer is more likely to take place than the formation of N_3O_3-ligated hexacoordinated species (**1a-Zn-6**), as hexacoordination is very rarely seen in the literature for Zn Schiff base complexes derived from aromatic diamines (e.g. Zn salphen complexes).[21] It should however be noted that octahedral Zn complexes of *reduced* hexadentate N_3O_3 Schiff base ligands are described in the literature,[22] and that hexacoordinated Zn complexes of tridentate Schiff base ligands are quite common.[23]

The presence of only one species in the ^{1}H NMR spectrum of **1a-Zn** in [D_6]DMSO, [D_7]DMF and [D_5]pyridine may be explained by ligation of a solvent molecule to Zn (Scheme 4).

The ligation of Lewis basic solvent molecules to Zn complexes of tetradentate Schiff base ligands is a characteristic attribute of their coordination chemistry.[5c,24] This ligation would inhibit the interconversions described in Scheme 3, as both the dimerization in **1a-Zn**–**D** and the coordination of the salicylaldimine group in **1a-Zn-5** depend on an open coordination site at Zn. The absence of a free coordination site at Zn would be expected to restrict the rotation around the C_{Ar}–C_{Ar} bond between rings A and A″ (Scheme 4) to a great extent, although the somewhat broadened ^{1}H NMR resonances of **1a-Zn** in [D_6]DMSO, [D_7]DMF and [D_5]pyridine suggest that the corresponding solvent-ligated complex does not possess a completely static conformation. Also, NOESY experiments of **1a-Zn** in [D_7]DMF at different temperatures suggest that several dynamic processes are taking place, as the imine protons H$^{d'}$ and H$^{d''}$ were found to exchange with each other at 27 °C (Scheme 5). Exchange peaks between the same resonances were not observed at −20 °C. For more details see Figure S140 and Figure S141, SI. The fluxional behaviour of **1a-Zn** in [D_7]DMF is similar to what has been reported for *m*-terpyridine[25] or pyridine[26] complexes of transition metals (e.g. Re(I) and Pt(IV)) in the literature.

In addition to complex **1a-Zn**, the related complex **1d-Zn** (Scheme 2) was studied by NMR. Complex **1d-Zn** behaved similar to **1a-Zn** in NMR, and two species (**1d-Zn-4** and **1d-Zn-5**) were observed in $CDCl_3$, in a ratio of 1.2:1 at ambient temperature. The interconversion between the two species could be observed in NOESY experiments (see Figure S162, SI), and the process depicted in Scheme 6 is suggested to be operative. Similar observations were made for the complex in C_6D_6.

The ^{1}H NMR resonances of **1d-Zn** in $CDCl_3$ were concentration-independent and sharp at ambient temperature. The ^{15}N NMR resonances corresponding to the imine nitrogen atoms of **1d-Zn-4** and **1a-Zn-5** in $CDCl_3$ could be obtained from ^{1}H-^{15}N HMBC experiments (Figure 5).

The ^{15}N NMR resonances corresponding to the two non-equivalent imine nitrogen atoms in ligand **1d** were observed at δ −126.9 and δ −119.6 ppm in $CDCl_3$. For **1d-Zn**, the ^{15}N NMR

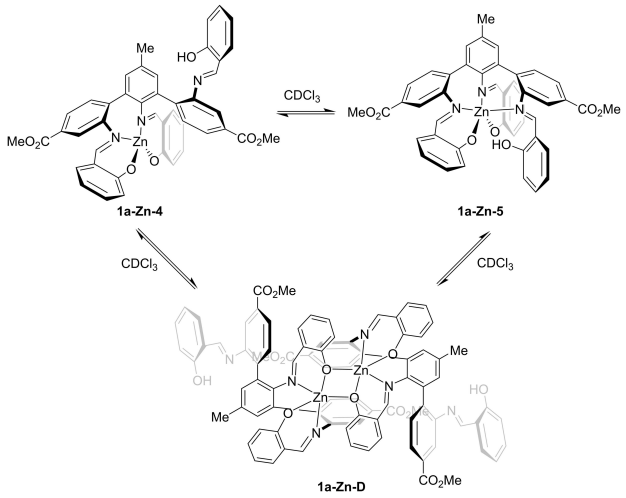

Scheme 3. Suggested interconversion of complex **1a-Zn** in $CDCl_3$.

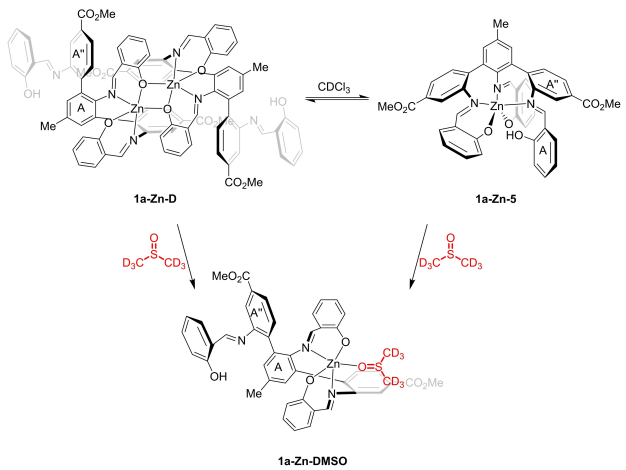

Scheme 4. Ligation of DMSO to complex **1a-Zn**. The ligation blocks the two tentative modes of pentacoordination seen for **1a-Zn** in $CDCl_3$, resulting in a more conventional ^{1}H NMR spectrum of the complex in [D_6]DMSO than in $CDCl_3$.

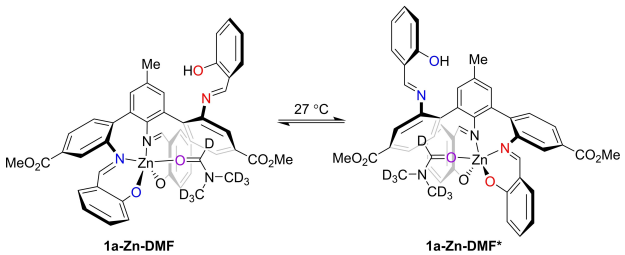

Scheme 5. Interconversion of **1a-Zn**–**DMF** and **1a-Zn**–**DMF*** at ambient temperature.

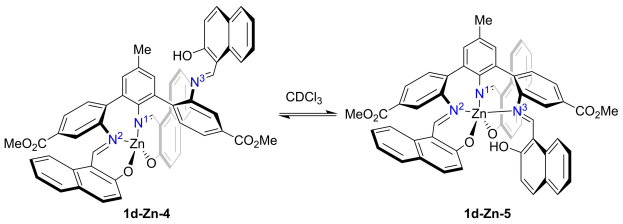

Scheme 6. Suggested dynamic behavior of the naphthol-derived complex **1d-Zn** in $CDCl_3$.

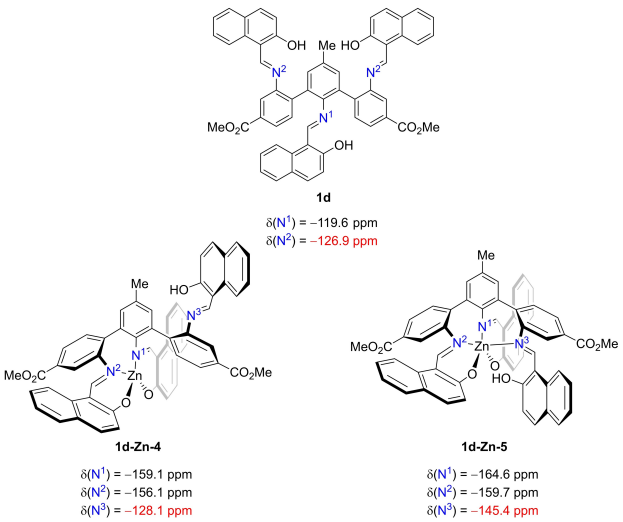

Figure 5. Overview of the ^{15}N NMR resonances found for **1d**, **1d-Zn-4** and **1d-Zn-5** in $CDCl_3$. Although resonances belonging to two different rotamers could be seen in the ^{1}H NMR and ^{13}C NMR spectra of ligand **1d**, their ^{15}N NMR resonances could not be differentiated.

resonances of the imine nitrogen atoms in the major species (**1d-Zn-4**) were found at δ −159.1, δ −156.1 and δ −128.1 for N^1, N^2 and N^3 respectively. The change to lower ppm values for the resonances corresponding to the coordinating imine nitrogen atoms (N^1 and N^2) is in accordance with what is expected when going from an uncoordinated nitrogen to a metal-coordinated nitrogen.[27] The resonance corresponding to the third imine nitrogen (N^3) in **1d-Zn** remained practically unchanged on comparison with the corresponding nitrogen in ligand **1d**, indicating that this nitrogen is not participating in any coordination. For N^3 in **1d-Zn-5** on the other hand, the corresponding ^{15}N NMR resonance was observed at a lower ppm value, δ −145.4, which indicates that N^3 may be participating in coordination to Zn. $\Delta\delta(N^3)$ is larger than what would be anticipated if the two different species observed in the ^{1}H NMR spectrum of **1d-Zn** were originating from restricted rotation around the C_{Ar}–C_{Ar} bond alone; it would then have been expected that similar differences in the ^{15}N NMR resonances of the two different rotamers of ligand **1d** could be observed, which was not the case.

Crystallographic structure determination of complexes 1a-Zn, 1d-Zn, 2a-Zn and 3-Zn

The four Zn complexes depicted in Scheme 2, **1a-Zn**, **1d-Zn**, **2a-Zn** and **3-Zn** were characterized by single-crystal X-ray diffraction analysis (Figure 6–Figure 9).

Both **1a-Zn** and **2a-Zn** crystallized as dimers, containing two pentacoordinated Zn centers with square pyramidal geometry, as evaluated by their τ_5 values[28] ($\tau_5 = 0.01$ for **1a-Zn**, and $\tau_5 = 0.04$ and 0.07 for **2a-Zn**). Complex **3-Zn** crystallized as the pentacoordinated monomer **3-Zn**–**MeOH**, with distorted trigonal bipyramidal geometry ($\tau_5 = 0.58$ and 0.65 for the two molecules of the asymmetric unit). For **1a-Zn** and **2a-Zn**, the Zn–μ-O bond distances were similar to what has been reported for a related dimeric Zn complex in literature.[17] The Zn–O-

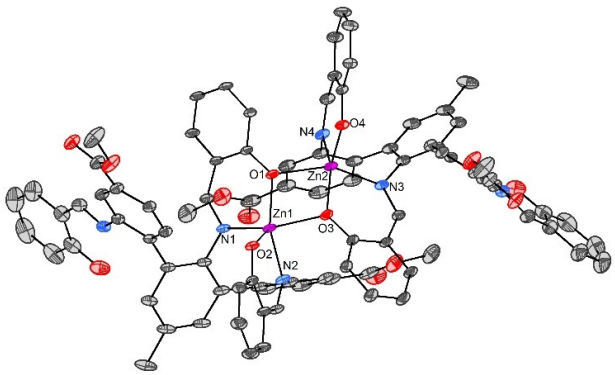

Figure 6. ORTEP plot of **1a-Zn** with 50% probability ellipsoids. Hydrogen atoms have been omitted for clarity. $\tau_5 = 0.01$. Selected bond lengths [Å] and angles [°]: Zn1–N1, 2.1644(18); Zn1–N2, 2.0316(16); Zn1–O1, 1.9592(13); Zn1–O2, 1.9300(15); Zn1–O3, 2.1480(16); N1–Zn1–N2, 87.22(7); N1–Zn1–O1, 88.47(6); N1–Zn1–O2, 108.79(7); N1–Zn1–O3, 147.54(6); N2–Zn1–O1, 148.19(7); N2–Zn1–O2, 94.95(7); N2–Zn1–O3, 92.01(7); O1–Zn1–O2; 116.22(6); O1–Zn1–O3, 75.35(6); O2–Zn1–O3, 103.61(6); Zn1–O1–Zn2, 101.53(6).

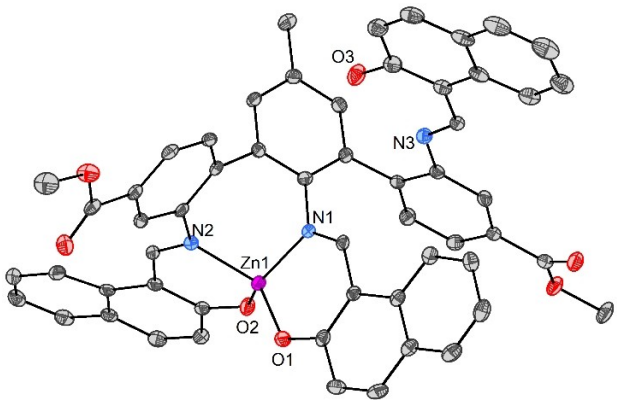

Figure 7. ORTEP plot of **1d-Zn** with 50% probability ellipsoids. Hydrogen atoms and non-coordinated solvents of crystallization (benzene and MeOH) have been omitted for clarity. $\tau_4' = 0.70$. Selected bond lengths [Å] and angles [°]: Zn1–N1, 1.9811(15); Zn1–N2, 2.0010(15); Zn1–O1, 1.9068(13); Zn1–O2, 1.9169(13); N1–Zn1–N2, 101.36(6); N1–Zn1–O1, 94.46(6); N1–Zn1–O2, 130.83(6); N2–Zn1–O1, 130.21(6); N2–Zn1–O2, 93.30(6); O1–Zn1–O2, 111.04(6).

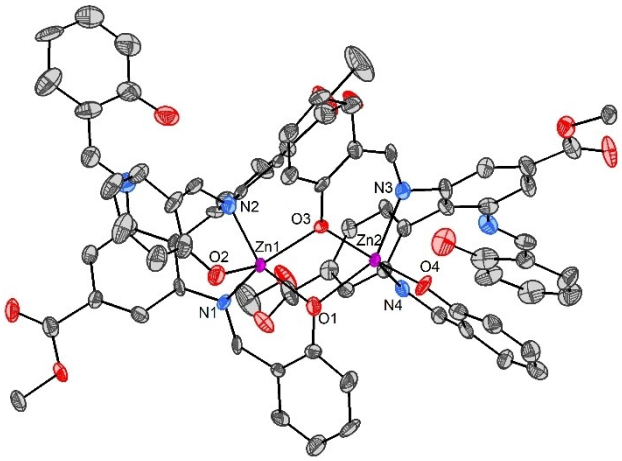

Figure 8. ORTEP plot of **2a-Zn** with 50% probability ellipsoids. Hydrogen atoms have been omitted for clarity. $\tau_5 = 0.07, 0.04$. Selected bond lengths [Å] and angles [°]: Zn1–N1, 2.210(9); Zn1–N2, 2.035(10); Zn1–O1, 1.946(8); Zn1–O2, 1.932(8); Zn1–O3, 2.172(7); Zn2–N3, 2.224(10); Zn2–N4, 2.027(9); Zn2–O1, 2.199(8); Zn2–O3, 1.955(7); Zn2–O4, 1.942(8); N1–Zn1–N2, 87.9(3); N1–Zn1–O1, 88.5(3); N1–Zn1–O2, 100.5(4); N1–Zn1–O3, 147.9(3); N2–Zn1–O1, 143.6(4); N2–Zn1–O2; 94.5(4); N2–Zn1–O3, 91.1(3); O1–Zn1–O2, 121.7(3); O1–Zn1–O3, 73.7(3); O2–Zn1–O3, 111.6(3); N3–Zn2–N4, 89.2(4); N3–Zn2–O1, 142.3(3); N3–Zn2–O3, 87.1(3); N3–Zn2–O4, 104.4(4); N4–Zn2–O1, 89.4(3); N4–Zn2–O3, 144.7(4); N4–Zn2–O4, 93.9(4); O1–Zn2–O3, 72.9(3); O1–Zn2–O4, 113.2(3); O3–Zn2–O4, 121.0(3); Zn1–O1–Zn2, 104.5(4); Zn1–O3–Zn2, 105.2(3).

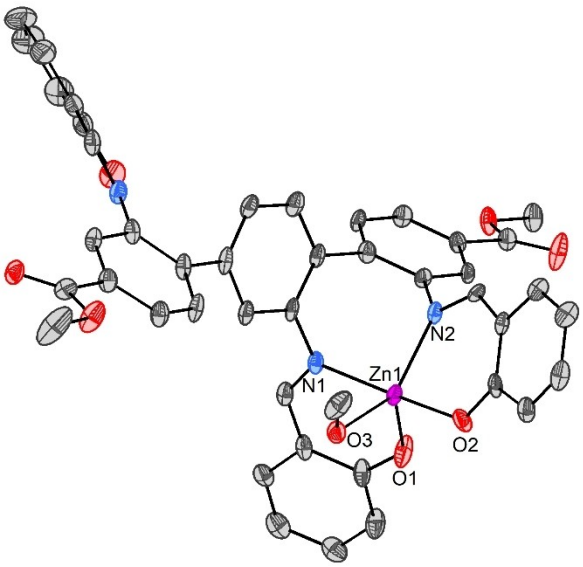

Figure 9. ORTEP plot of **3**–**Zn**–**MeOH** with 50% probability ellipsoids. Only one of the two molecules of the asymmetric unit is displayed, but metric data for both are given below. Hydrogen atoms and CH_2Cl_2 (solvent of crystallization) have been omitted for clarity. $\tau_5 = 0.58, 0.65$. Selected bond lengths [Å] and angles [°]: Zn1–N1, 2.100(3); Zn1–N2, 2.072(3); Zn1–O1, 1.922(3); Zn1–O2, 1.999(2); Zn1–O3, 2.126(3); Zn2–N3, 2.098(3); Zn2–N4, 2.072(3); Zn2–O4, 1.941(2); Zn2–O5, 1.996(3); Zn2–O6, 2.160(2); N1–Zn1–N2, 90.84(11); N1–Zn1–O1, 90.62(11); N1–Zn1–O2, 169.04(11); N1–Zn1–O3, 84.45(10); N2–Zn1–O1, 117.23(12); N2–Zn1–O2, 89.15(11); N2–Zn1–O3, 134.14(11); O1–Zn1–O2, 99.12(12); O1–Zn1–O3, 108.44(12); O2–Zn1–O3, 87.70(10); N3–Zn2–N4, 92.08(11); N3–Zn2–O4, 89.79(11); N3–Zn2–O5, 168.34(10); N3–Zn2–O6, 84.41(10); N4–Zn2–O4, 117.03(11); N4–Zn2–O5, 90.81(11); N4–Zn2–O6, 129.10(10); O4–Zn2–O5, 98.95(10); O4–Zn2–O6, 113.73(10); O5–Zn2–O6, 85.00(9).

(MeOH) bond length for **3-Zn–MeOH** (Zn1–O3, 2.126(3) Å) is comparable with reported Zn–O bond lengths in the literature for a EtOH-ligated Zn Schiff base complex,[29] but longer than the Zn–O(MeOH) bond in a MeOH-ligated Zn salphen complex.[30] Although NMR studies suggested the presence of a potential pentacoordinated species, naphthol-derived **1d-Zn** crystallized as a tetracoordinated complex with distorted tetrahedral geometry around Zn, as evaluated by its τ_4' value[31] of 0.70. The distorted geometry and the Zn–N and Zn–O bond lengths are in accordance with observations for related tetracoordinated Zn Schiff base complexes in the literature.[14,32]

Synthesis and characterization of 1a-Co(acac), 1d-Co(acac) and 8-Co(acac)

The ^{1}H NMR spectra of **1a-Zn** and **1d-Zn** in $CDCl_3$ showed the presence of two (interconvertible) species for each complex. To rationalize that this phenomenon was caused by the flexible nature of Zn with respect to ligand substitution reactions, as well as changes in coordination geometries and numbers, the corresponding Co(III) complexes **1a-Co(acac)** and **1d-Co(acac)** were synthesized for comparative NMR studies (Scheme 7). As opposed to Zn(II) complexes, low-spin octahedral Co(III) complexes are known for being kinetically inert, and in the ^{1}H NMR spectra of **1a-Co(acac)** and **1d-Co(acac)** in $CDCl_3$, sharp and well-defined resonances were observed, being in stark contrast to the ^{1}H NMR spectrum of e.g. **1a-Zn** in $CDCl_3$ at comparable concentrations. Furthermore, for the Co(acac) complexes, only one species was observed, while for **1a-Zn** and **1d-Zn**, two

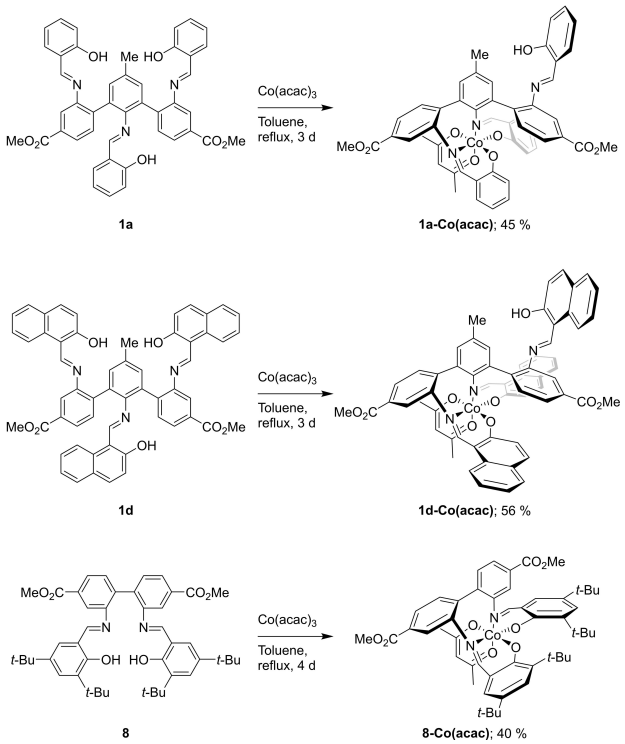

Scheme 7. Synthesis of complexes **1a-Co(acac)**, **1d-Co(acac)**, and **8-Co(acac)**.

species could be observed. This suggest that the accessibility of an open coordination site at the metal center dictates how the ^{1}H NMR spectrum of the corresponding complex will appear.

Complex **1d-Co(acac)** was characterized by single-crystal X-ray diffraction analysis (Figure 10), and crystallized with the expected octahedral geometry around Co. Ligand **1d** acted as a tetradentate N_2O_2 ligand, occupying three of the equatorial and one of the axial sites around Co. The bidentate acac ligand concluded the coordination sphere around Co. Overall, the bond angles and bond lengths in structure of **1d-Co(acac)** were found to be similar to those reported by Shi and Duan for a similar Co(III) complex derived from 1,1′-binaphthalene-2,2′-diamine.[33] In addition to **1a-Co(acac)** and **1d-Co(acac)**, a related complex, **8-Co(acac)**, was synthesized (Scheme 7, lower part). The complex was also crystallographically characterized (see SI), showing very similar geometry around Co as that observed for **1d-Co(acac)**.

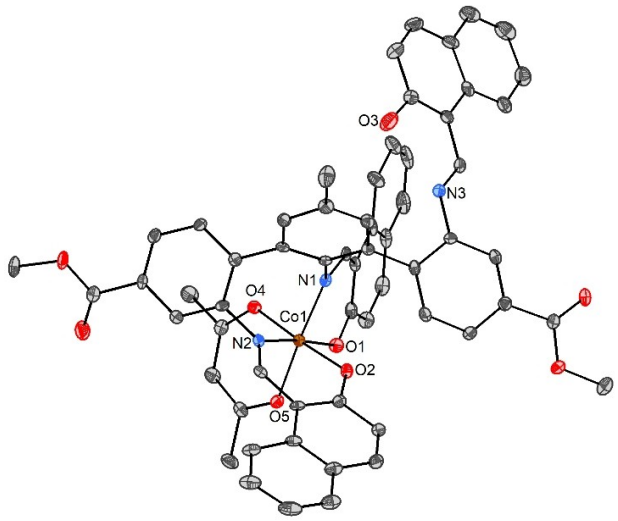

Figure 10. ORTEP plot of **1d-Co(acac)** with 50% probability ellipsoids. Hydrogen atoms and non-coordinated solvents of crystallization (benzene and MeCN) have been omitted for clarity. Selected bond lengths [Å] and angles [°]: Co1–N1, 1.925(4); Co1–N2, 1.902(4); Co1–O1, 1.889(3); Co1–O2, 1.871(3); Co1–O4, 1.891(3); Co1–O5, 1.892(3); N1–Co1–N2, 92.46(16); N1–Co1–O1, 92.96(15); N1–Co1–O2, 90.12(15); N1–Co1–O4, 87.50(15); N1–Co1–O5, 175.84(15); N2–Co1–O1, 174.57(16); N2–Co1–O2, 91.82(16); N2–Co1–O4, 92.09(15); N2–Co1–O5, 88.67(15); O1–Co1–O2, 88.60(14); O1–Co1–O4, 87.72(14); O1–Co1–O5, 85.96(14); O2–Co1–O4, 175.50(14); O2–Co1–O5, 85.85(14); O4–Co1–O5, 96.46(14).

Synthesis and NMR studies of Zn complex 1b-Zn–NH_2

In addition to ligands **1a** and **1d**, the reactivity of the nitro-substituted ligand **1b** towards Zn was studied. Ligand **1b** was found to behave different from **1a** and **1d** when it was reacted with $Zn(OAc)_2 \cdot 2H_2O$ in the presence of NEt_3 in a solution of CH_2Cl_2 and MeOH (Scheme 8). For **1b**, only two imine functionalities were intact in the corresponding product **1b-Zn–NH_2**, as the third imine hydrolyzed and left behind an NH_2 group. From the single-crystal X-ray diffraction analysis of the complex, the NH_2 group was found to coordinate to Zn (*vide infra*). The fluorine-substituted ligand **1c** did not react cleanly with $Zn(OAc)_2 \cdot 2H_2O$ under similar conditions as those described for **1a**, **1b** and **1d**, and a mixture of products was obtained instead (see SI for details).

The partial hydrolysis of imines in complexation of Schiff base ligands is occasionally reported in the literature,[34] leading to metal complexes of mixed amine-imine ligands. NMR characterization of **1b-Zn–NH_2** was mainly conducted in [D_6]DMSO, due to the poor solubility of the complex in e.g. $CDCl_3$. Nevertheless, limited ^{1}H NMR studies could be performed in $CDCl_3$ (*vide infra*). In [D_6]DMSO, two species were observed. The two species were determined to be interconvertible from NOESY and variable-temperature ^{1}H NMR experiments. From the crystal structure determination of the complex (*vide infra*) it was found that the Zn–NH_2 bond (2.177(2) Å) was approximately in the same range as the Zn–μ-O bonds that were found from the single-crystal X-ray diffraction analysis of **1a-Zn** and **2a-Zn**. In addition, the Zn–NH_2 bond in **1b-Zn–NH_2** was of similar length as the Zn–O(DMSO) bond in a related Zn complex previously reported by us.[17] As [D_6]DMSO is susceptible to break up dimeric pentacoordinated Zn Schiff base complexes and form monomeric pentacoordinated DMSO-ligated complexes, the same may occur for **1b-Zn–NH_2**. However, since the nature of the pentacoordination for the latter is predominantly intramolecular, DMSO ligation would be less favorable compared to dimers where the pentacoordination at Zn is a result of an intermolecular process. This may explain the presence of two interconvertible species in the ^{1}H NMR spectrum of **1b-Zn–NH_2** in [D_6]DMSO (Scheme 9), as opposed to e.g. **2a-Zn**, for which only one species could be detected in the ^{1}H NMR spectrum of the complex in [D_6]DMSO.

In the ^{1}H NMR spectrum of **1b-Zn–NH_2** in [D_6]DMSO, the differences in the resonances of the major species and the corresponding resonances of the minor species were in some

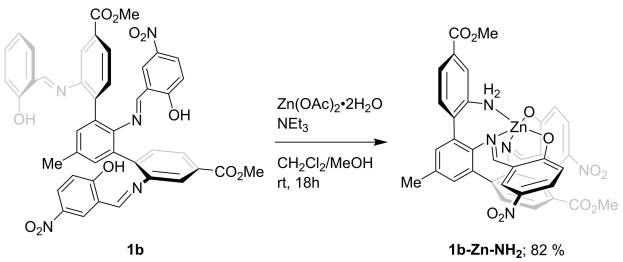

Scheme 8. Synthesis of complex **1b-Zn–NH_2**.

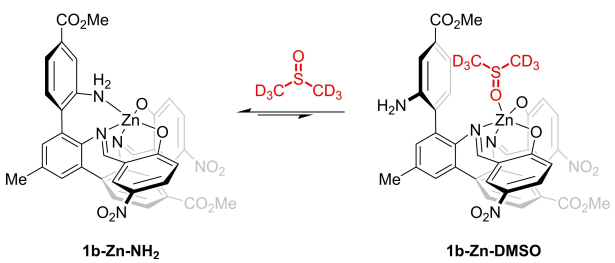

Scheme 9. Proposed partial solvolysis of **1b-Zn–NH_2** in [D_6]DMSO.

cases rather large. This was especially evident for the resonances corresponding to the protons of the NH_2-substituted ring, as well as the NH_2 protons (Figure 11). For the major component, the resonances corresponding to the three ring protons $H^{a''}$, $H^{b''}$ and $H^{c''}$ were observed at relatively high ppm values, at δ 7.94–7.96, δ 7.58–7.59 and δ 7.48 respectively, and the resonance corresponding to the NH_2 protons was observed at δ 6.17. In the minor component, the ^1H NMR resonances of the protons of discussion were observed at significantly lower ppm values; δ 7.27, δ 7.00, δ 6.82 and δ 5.16 respectively, being closer to what is expected for an aromatic amine of this kind.[17]

The ^{15}N NMR resonance of the NH_2 nitrogen of the major component was observed at a lower ppm value than the corresponding resonance of the minor component (δ −326.9 and δ −317.2 respectively) (Figure 12). This can be seen as an indication that the major component in [D_6]DMSO actually is the NH_2-coordinated complex depicted to the left in Scheme 9.[27c–d] The ^{15}N NMR resonances of **1b-Zn–NH$_2$** were compared to those of triamine **5**. From ^1H-^{15}N HMBC of **5** in [D_6]DMSO, the ^{15}N NMR resonance corresponding to the "outer" NH_2 nitrogen (N^2H_2 in Figure 12) could be assigned. The ppm value was found to be comparable to the corresponding amino nitrogen in the minor species observed for **1b-Zn–NH$_2$**, yet another indication of the coordination of the amino group in the major species.

In the ^1H NMR spectrum of **1b-Zn–NH$_2$** in $CDCl_3$, only one species was observed (Figure 13). All the ^1H NMR resonances belonging to the NH_2-substituted ring in **1b-Zn–NH$_2$** were found at relatively high ppm values in $CDCl_3$ (δ 7.82, δ 7.70 and δ 7.51–7.53 for $H^{b''}$, $H^{a''}$ and $H^{c''}$ respectively), similar to what was observed for the major component in [D_6]DMSO. This indicates that the pentacoordinated complex might be intact in $CDCl_3$. The resonance corresponding to $H^{a'}$ of **1b-Zn–NH$_2$** in $CDCl_3$ was observed at δ 7.72, which is more upfield than what was reported for the corresponding ^1H NMR resonances of Zn Schiff base complexes derived from biphenyl-2,2′-diamines at approximately the same concentration (typically δ 7.80–7.85 at ca. $2.6\cdot10^{-3}$ M).[14] As the chemical shift of this specific resonance was found to be useful for the assignment of coordination numbers of these Zn complexes in $CDCl_3$, the more upfield ^1H NMR resonance of $H^{a'}$ in **1b-Zn–NH$_2$** indicates that Zn is not tetracoordinated, further strengthening the assumption that **1b-Zn–NH$_2$** remains pentacoordinated in $CDCl_3$. The differences observed in the ^1H NMR spectra of **1b-Zn–NH$_2$** as a function of the donating ability of the solvents used, are consistent with those observed for a Ru(II) complex bearing a 6,6′-diamino-2,2′-bipyridine ligand in the literature, where the amino groups were observed to dissociate in CD_3CN but remaining ligated in CD_2Cl_2.[35]

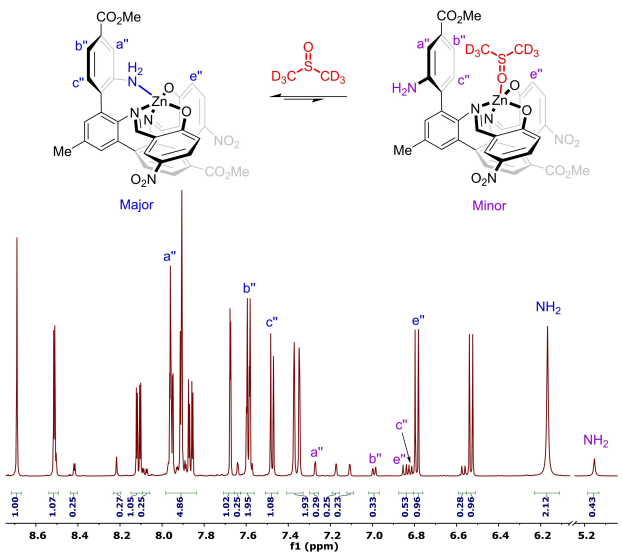

Figure 11. ^1H NMR (600 MHz, [D_6]DMSO) spectrum of **1b-Zn–NH$_2$** showing the aromatic region as well as NH_2 protons. Only the assignments that are discussed in the text are shown.

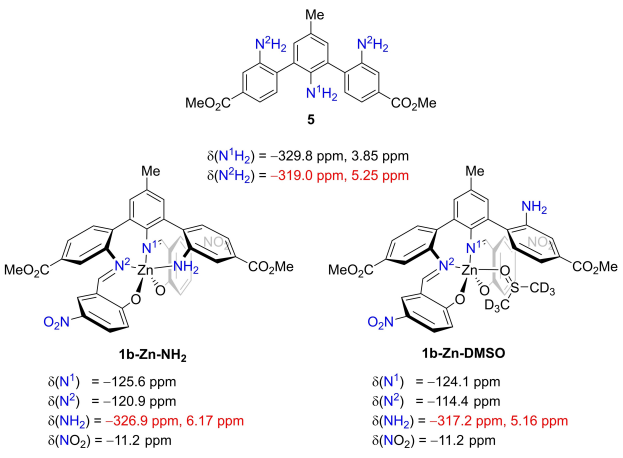

Figure 12. Overview of the ^{15}N NMR resonances found for **5**, **1b-Zn–NH$_2$** and **1b-Zn–DMSO** in [D_6]DMSO. Only the ^1H NMR and ^{15}N NMR resonances corresponding to the NH_2 group of the major rotamer of **5** is included.

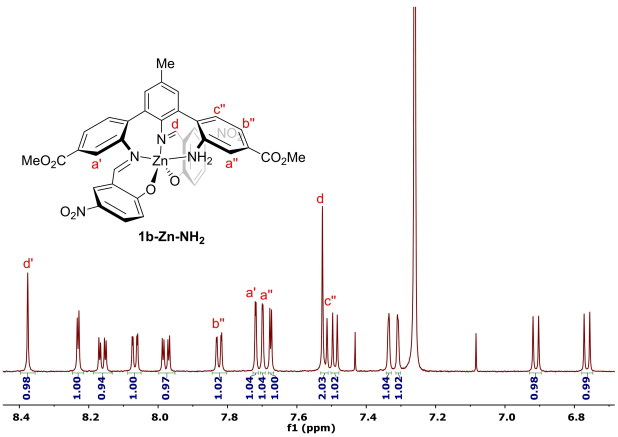

Figure 13. ^1H NMR (600 MHz, $CDCl_3$) spectrum of **1b-Zn–NH$_2$** ($2.6\cdot10^{-3}$ M) showing the aromatic region.

Synthesis and NMR studies of Cd complex 1b-Cd–NH_2

In light of the unexpected outcome of the reaction between **1b** and $Zn(OAc)_2 \cdot 2H_2O$, the reactivity of ligand **1b** towards $Cd(OAc)_2 \cdot 2H_2O$ was investigated (Scheme 10).

The resulting Cd complex was investigated by NMR spectroscopy, in addition to single-crystal X-ray diffraction analysis (*vide infra*), and **1b-Cd–NH_2** was found to crystallize as a dimer, with hexacoordination around both Cd atoms. Analogously to the Zn complex, the ^{1}H NMR spectrum of **1b-Cd–NH_2** in [D_6]DMSO revealed a mixture of two interconvertible species. At ambient temperature, the ratio between these species was 2:1 in favor the NH_2-coordinated species for **1b-Cd–NH_2**, compared to 6:1 for the Zn complex. The resonance corresponding to the NH_2 protons of the major component showed subtle splitting that could indicate coordination to Cd (Figure 14).

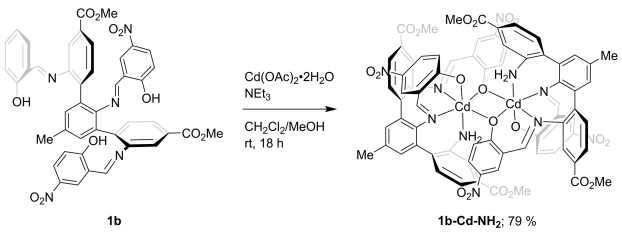

Scheme 10. Synthesis of Cd complex **1b-Cd–NH_2**.

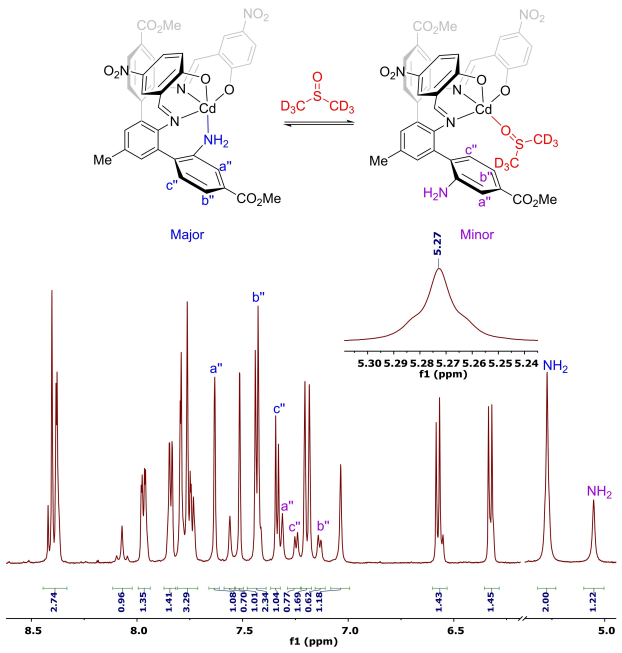

Figure 14. ^{1}H NMR (600 MHz, [D_6]DMSO) spectrum of **1b-Cd–NH_2** showing the aromatic region and the amino protons. Only the assignments of the protons discussed in the text are shown. The Cd complexes are depicted as pentacoordinated monomers for simplicity. The insert shows the subtle splitting of the resonance corresponding to the NH_2 protons of the major species.

As for **1b-Zn–NH_2**, the largest differences in ppm values for the major and the minor component in [D_6]DMSO were found for the protons of the NH_2-substituted aromatic ring. However, the differences found for **1b-Cd–NH_2** were significantly smaller than what was found for **1b-Zn–NH_2**. For **1b-Cd–NH_2**, $\Delta\delta$ between the major and the minor species was 0.32, 0.29, 0.07 and 0.22 for $H^{a''}$, $H^{b''}$, $H^{c''}$ and NH_2 respectively, whereas $\Delta\delta$ was 0.68, 0.58, 0.66 and 1.01 for **1b-Zn–NH_2**. From these observations, the internal NH_2 coordination in **1b-Cd–NH_2** in [D_6]DMSO seems more labile than that in **1b-Zn–NH_2**, which was further supported by observations from ^{1}H-^{15}N HMBC experiments. The ^{15}N NMR resonances corresponding to the NH_2 nitrogen atoms of the two species were observed at δ −322.8 and δ −318.9 respectively, being closer to each other than what was found for **1b-Zn–NH_2** (Figure 15). This was further illustrated by relatively long Cd–NH_2 bonds in **1b-Cd–NH_2** (2.470(12) Å and 2.418(12) Å) found from the crystal structure determination of the complex (*vide infra*).

The increased lability of the NH_2-coordination in **1b-Cd–NH_2** compared to **1b-Zn–NH_2** was further supported by variable-temperature ^{1}H NMR experiments performed in [D_6]DMSO. The two NH_2-resonances in Figure 14 had coalesced at 77 °C for **1b-Cd–NH_2**, whereas two distinct resonances still could be observed for **1b-Zn–NH_2** at the same temperature. In addition, the Cd complex was found to undergo significant decomposition when exposed to elevated temperatures in [D_6]DMSO, while the Zn complex showed no signs of degradation. For more details, see Figure S146–S147 (**1b-Zn–NH_2**), and Figure S209–S210 (**1b-Cd–NH_2**), SI. Attempts of synthesizing a Hg(II) complex of ligand **1b** employing the conditions described for the synthesis of **1a-Zn–NH_2** and **1b-Cd–NH_2** did not yield a conclusive outcome.

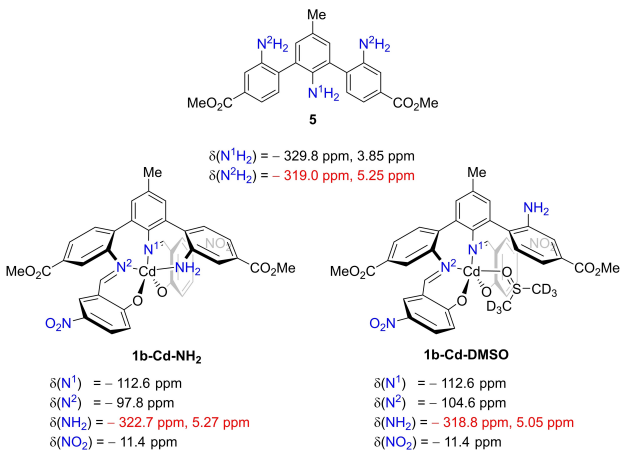

Figure 15. Overview of the ^{15}N NMR resonances found for **5**, **1b-Cd–NH_2** and **1b-Cd–DMSO** in [D_6]DMSO. The Cd complexes are depicted as pentacoordinated monomeric species for simplicity. Only the ^{1}H NMR and ^{15}N NMR resonances corresponding to the NH_2 group of the major rotamer of **5** is included.

Synthesis and characterization of Ni complex 9-Ni, and Cu complexes 1b-Cu–NH_2, 1a-Cu–NH_2 and 9-Cu.

Whereas Zn(II) and Cd(II) share many similarities in terms of coordination chemistry, Cd(II) is considerably larger than Zn(II). Cu(II) and Ni(II) on the other hand, both have a more similar ionic radius to Zn(II). To investigate Cu(II) and Ni(II) Schiff base complexes derived from biphenyl-2,2′-diamines, complexes **9-Cu** and **9-Ni** were prepared (Scheme 11).

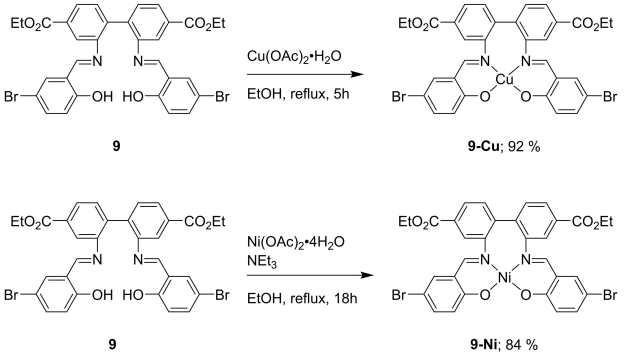

Scheme 11. Synthesis of **9-Cu** and **9-Ni**. The Ni(II) complex is depicted as tetracoordinated monomer for simplicity.

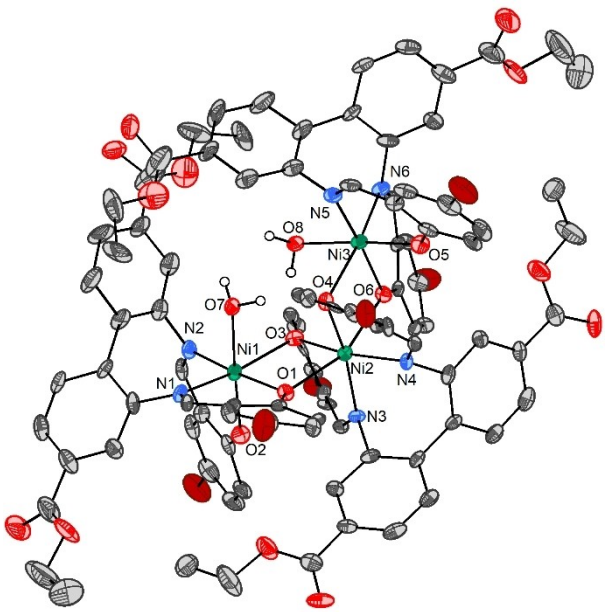

Figure 16. ORTEP plot of **9**–**Ni** with 50 % probability ellipsoids. Hydrogen atoms (except those of the water ligands) and non-coordinated, disordered solvent molecules have been omitted for clarity. Selected bond lengths [Å] and angles [°]: Ni1–N1, 2.034(6); Ni1–N2, 2.011(6); Ni1–O1, 2.025(5); Ni1–O2, 1.995(5); Ni1–O3, 2.137(5); Ni1–O7, 2.169(5); Ni2–N3, Ni2–N4, 2.059(6); Ni2–O1, Ni2–O6, 2.144(5); Ni2–O3, Ni2–O4, 2.065(5); N1–Ni1–N2, 92.6(2); N1–Ni1–O1, 93.2(2); N1–Ni1–O2, 95.2(2); N1–Ni1–O3, 167.2(2); N1–Ni1–O7, 84.9(2); N2–Ni1–O1, 174.2(2); N2–Ni1–O2, 89.4(2); N2–Ni1–O3, 92.6(2); N2–Ni1–O7, 95.2(2); O1–Ni1–O2, 90.1(2); O1–Ni1–O3, 81.69(18); O1–Ni1–O7, 85.23(19); O2–Ni1–O3, 96.48(16); O2–Ni1–O7, 175.4(2); O3–Ni1–O7, 83.03(18); Ni1–O3–Ni2, 98.06(19); Ni1–O1–Ni2, 99.14(18); N3–Ni2–N4, 92.3(3); N3–Ni2–O1, N4–Ni2–O6, 82.9(5); N3–Ni2–O3, N4–Ni2–O4, 86.4(2); N3–Ni2–O4, N4–Ni2–O3, 166.3(2); N3–Ni2–O6, N4–Ni2–O1, 112.8(2); O1–Ni2–O3, O4–Ni2–O6, 80.62(18); O1–Ni2–O4, O3–Ni2–O6, 85.03(18); O1–Ni2–O6, 158.1(3); O3–Ni2–O4, 98.0(3).

The Ni(II) complex was analyzed by MS, elemental analysis and single-crystal X-ray diffraction, in addition to ^{1}H NMR studies in different solvents ($CDCl_3$, C_6D_6 and [D_6]DMSO). A paramagnetic species was consistently observed, with severe line-broadening of the resonances. Magnetic moment measurement of **9-Ni** in $CDCl_3$ at 25 °C using Evans method,[36] gave $\mu_B =$ 2.23, which is lower than expected for Ni(II) with 2 unpaired electrons ($\mu_B = 2.9–4.0$).[37] This may be indicative of interconversion between different geometries in solution, which is occasionally reported for Ni Schiff base complexes in the literature.[36b,38] Recrystallization of **9-Ni** from benzene gave crystals suitable for single-crystal X-ray diffraction analysis. The complex crystallized as a trimer, with two unique Ni centers, both having distorted octahedral geometry (Figure 16).

For the middle Ni center in **9-Ni** (Ni2), one molecule of the Schiff base ligand was found to coordinate in a $N_2O_2^{2-}$ tetradentate fashion, whereas the two other Schiff base ligands in the structure contributed with one bridging oxygen ligand each (O1 and O6 respectively), resulting in the observed hexacoordination around Ni2. For the terminal Ni centers (Ni1 and Ni3), the coordination sphere around each Ni atom was made up from one Schiff base ligand acting as a $N_2O_2^{2-}$ tetradentate ligand. The two last coordination sites were occupied by a water ligand, and one bridging oxygen ligand from the Schiff base moiety binding the middle metal center, Ni2. For the two unique Ni centers in the crystal structure, Ni2 was observed to have a more distorted octahedral geometry than Ni1/Ni3.

The synthesis of Cu(II) complex **9-Cu** was carried out according to literature protocols.[38a] The complex was characterized by MS, elemental analysis, UV-Vis (*vide infra*) and single-crystal X-ray diffraction analysis. Single-crystal X-ray diffraction analysis revealed that the Cu complex crystallized as a tetracoordinated monomer even from a mixture of two strongly coordinating solvents, DMSO and MeCN (Figure 17).

For **9-Cu**, a distorted square planar geometry was observed ($\tau_4' = 0.43$). The bond lengths and angles between Cu and the donor atoms of the ligand were similar to those reported in the literature for related Cu(II) complexes.[38a,39] The observed tetracoordination around Cu in **9-Cu** is interesting as it indicates that pentacoordination is less favored for Cu(II) than for Zn(II) in complexes of Schiff base ligands derived from biphenyl- and terphenyl-2,2′-diamines; Zn complexes of this type of ligands readily form DMSO-ligated adducts when recrystallized from DMSO.[14,17] To further investigate these apparent differences between Cu(II) and Zn(II), the reactivity of ligand **1b** towards Cu(II) was studied, as this specific ligand facilitated the formation of a pentacoordinated complex for Zn(II). In addition, the combination of a redox active metal, e.g. Cu, and an amine in proximity can make a catalyst candidate in reactions where both electron and proton transfers are essential.[15b–c,40] The attempted synthesis of **1b-Cu–NH_2** was carried out according to the procedure for **1b-Zn–NH_2** and **1b-Cd–NH_2**. From MS analysis of the product from the reaction of **1b** with Cu-$(OAc)_2 \cdot H_2O$, *m/z* values corresponding to both **1b-Cu–NH_2** and

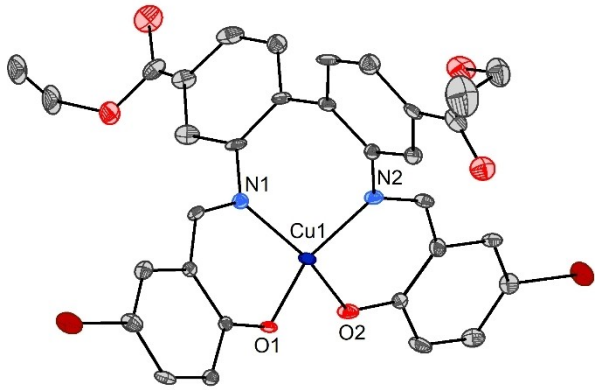

Figure 17. ORTEP plot of **9**–**Cu** with 50 % probability ellipsoids. Only one of the two molecules of the asymmetric unit is displayed, but metric data for both are given below. Hydrogen atoms, non-coordinated MeCN (solvent of crystallization) and disorder in one of the ethoxycarbonyl substituents have been omitted for clarity. $\tau_4' = 0.43, 0.43$. Selected bond lengths [Å] and angles [°]: Cu1–N1, 1.952(6); Cu1–N2, 1.951(6); Cu1–O1, 1.896(5); Cu1–O2, 1.897(5); Cu2–N3, 1.955(5); Cu2–N4, 1.950(6); Cu2–O3, 1.886(5); Cu2–O4, 1.900(5); N1–Cu1–N2, 96.8(2); N1–Cu1–O1, 93.7(2); N1–Cu1–O2, 150.4(2); N2–Cu1–O1, 148.1(2); N2–Cu1–O2, 93.5(2); O1–Cu1–O2, 92.1(2); N3–Cu2–N4, 97.0(2); N3–Cu2–O3, 93.7(2); N3–Cu2–O4, 149.8(2); N4–Cu2–O3, 149.9(2); N4–Cu2–O4, 94.8(2); O3–Cu2–O4, 89.8(2).

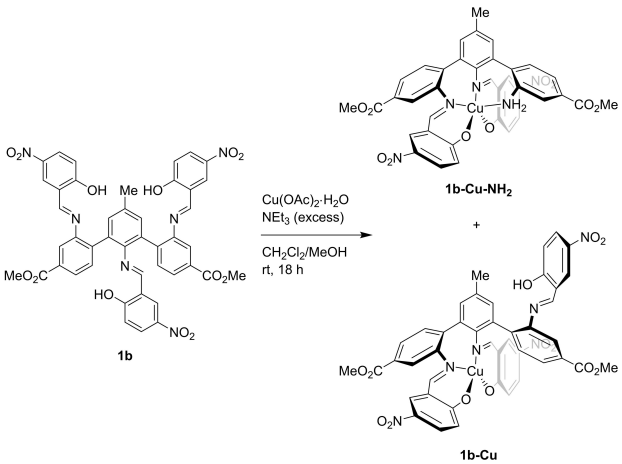

Scheme 12. Attempted synthesis of **1b**-**Cu**–$\mathbf{NH_2}$. A mixture of **1b**-**Cu**–$\mathbf{NH_2}$ and **1 b**-**Cu** was obtained.

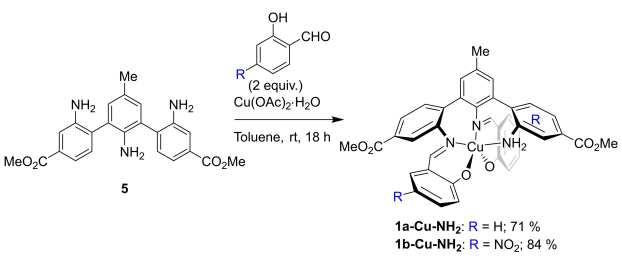

Scheme 13. Synthesis of **1a**-**Cu**–$\mathbf{NH_2}$ and **1b**-**Cu**–$\mathbf{NH_2}$ directly from triamine **5** using a one-pot procedure.

the complex **1b**-**Cu**, with a fully intact ligand, were observed (Scheme 12), indicating that the reactivity of ligand **1b** is highly metal-dependent, even for Cu(II) and Zn(II), which are similarly sized and Lewis acidic.

Whereas the method depicted in Scheme 12 proved unsuccessful for the selective synthesis of **1b**-**Cu**–$\mathbf{NH_2}$, the compound as well as the related complex **1a**-**Cu**–$\mathbf{NH_2}$ could be synthesized directly from triamine **5**, 2 equivalents of the corresponding salicylaldehyde derivative and $Cu(OAc)_2 \cdot H_2O$ (Scheme 13).

In addition to single-crystal X-ray diffraction analysis (*vide infra*), **1b**-**Cu**–$\mathbf{NH_2}$ and **1a**-**Cu**–$\mathbf{NH_2}$ were characterized by MS, UV/Vis and elemental analysis. The UV-Vis spectra of the two complexes, alongside the previously discussed complex **9**-**Cu** are shown in Figure 18.

The UV/Vis absorption spectra show defined bands at 365 nm, 399 nm and 410 nm for **1b**-**Cu**–$\mathbf{NH_2}$, **1a**-**Cu**–$\mathbf{NH_2}$ and **9**-**Cu** respectively, which could be attributed to ligand-to-metal charge transfer from the phenoxide donors in the ligands to the Cu(II) center, based on observations in the literature concerning related complexes.[41] Of the three complexes, the absorption band of nitro-substituted **1b**-**Cu**–$\mathbf{NH_2}$ was slightly more blue-shifted and significantly more intense than the corresponding bands for **1a**-**Cu**–$\mathbf{NH_2}$ and **9**-**Cu**. Similar observations were made by Decinti and co-workers on comparison of a nitro-substituted chiral Cu salen complex with a non-substituted complex.[42] Very intense absorption bands were observed at $\lambda < 300$ nm for **1b**-**Cu**–$\mathbf{NH_2}$, **1a**-**Cu**–$\mathbf{NH_2}$ and **9**-**Cu**, which may be attributed to $\pi \rightarrow \pi^*$ transitions associated with the ligands. Low-intensity ligand field (d→d) transitions were observed between 651 nm and 687 nm for the three complexes, with the bands associated with **1b**-**Cu**–$\mathbf{NH_2}$ and **1a**-**Cu**–$\mathbf{NH_2}$ being more broadened than that of **9**-**Cu** (see insert in Figure 18).

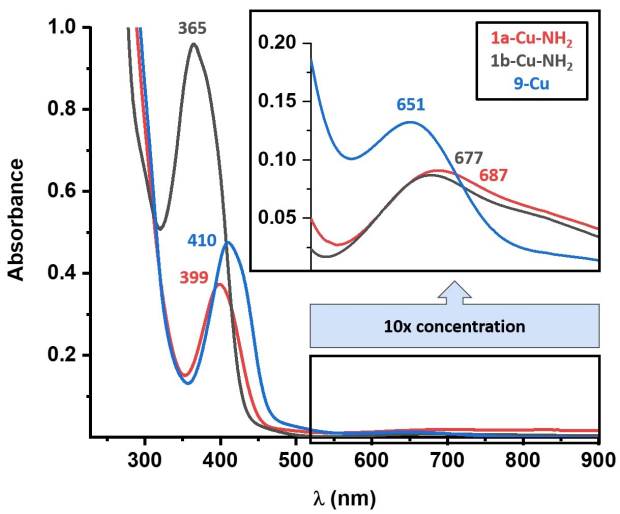

Figure 18. UV/Vis (CH_2Cl_2) spectra of Cu(II) complexes **1b**-**Cu**–$\mathbf{NH_2}$, **1a**-**Cu**–$\mathbf{NH_2}$ and **9**–**Cu** at similar concentrations.

Crystallographic structure determination of 1b-Zn–NH_2, 1b-Cd–NH_2, 1b-Cu–NH_2, and 1a-Cu–NH_2

Complexes **1b-Zn–NH_2**, **1b-Cd–NH_2**, **1b-Cu–NH_2** and **1a-Cu–NH_2** were characterized by single-crystal X-ray diffraction analysis (Figure 19, Figure 20, Figure 21 and Figure 22).

All four complexes crystallized with the NH_2 group coordinating to the metal. Whereas the Zn complex and the two Cu complexes crystallized as pentacoordinated monomers, the Cd complex crystallized as a dimer with distorted octahedral geometries around both Cd atoms. The geometry found for **1b-Cu–NH_2** was distorted trigonal bipyramidal ($\tau_5 = 0.70$), while distorted square pyramidal geometries were found for both **1b-Zn–NH_2** ($\tau_5 = 0.33$) and **1a-Cu–NH_2** ($\tau_5 = 0.25$). The bond distance between Zn and the amino group in **1b-Zn–NH_2** is comparable to literature values for Zn–NH_2 bond distances.[43] In **1b-Cd–NH_2**, the bonds between the Cd atoms and the NH_2 groups (Cd1–N3 and Cd2–N6) are rather long (2.470(12) Å and 2.418(12) Å respectively), and significantly longer than the corresponding Zn–N bond in **1b-Zn–NH_2** (2.177(2) Å), as anticipated from the NMR comparisons of the two complexes (*vide supra*). Similarly, the Cd–μ-O bonds (Cd1–O4, 2.315(10) Å and Cd2–O2, 2.329(10) Å) are considerably longer than the corresponding Zn–O bonds in e.g. dimeric **1a-Zn** (2.1480(16) Å), and of similar length as Cd–μ-O bonds in multinuclear Cd Schiff base complexes reported in the literature.[10b,14,44] Although relatively rare, there are a few reported examples of coordination compounds of Cd where one of the ligands is an aromatic amine, and the observed Cd–NH_2 bond distances in **1b-Cd–NH_2** are in accordance with those reported in literature.[43a–b,45]

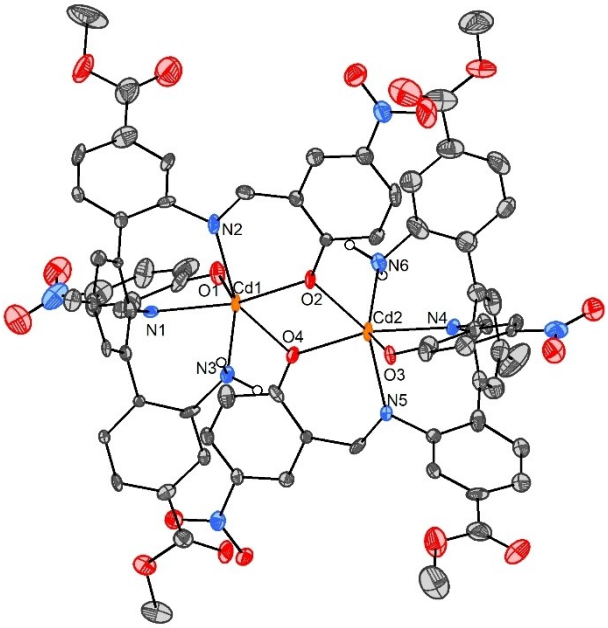

Figure 20. ORTEP plot of **1b-Cd–NH_2** with 50% probability ellipsoids. Hydrogen atoms (except for NH_2) and non-coordinated MeOH (solvent of crystallization) have been omitted for clarity. Selected bond lengths [Å] and angles [°]: Cd1–N1, 2.300(11); Cd1–N2, 2.363(13); Cd1–N3, 2.470(12); Cd1–O1, 2.249(11); Cd1–O2, 2.248(9); Cd1–O4, 2.315(10); Cd2–N4, 2.299(12); Cd2–N5, 2.358(12); Cd2–N6, 2.418(12); Cd2–O2, 2.329(10); Cd2–O3, 2.301(10); Cd2–O4, 2.273(9); N1–Cd1–N2, 81.0(4); N1–Cd1–N3, 80.7(4); N1–Cd1–O1, 78.9(4); N1–Cd1–O2; 157.0(4); N1–Cd1–O4, 126.3(4); N2–Cd1–N3, 118.1(4); N2–Cd1–O1, 86.0(4); N2–Cd1–O2, 81.1(4); N2–Cd1–O4, 149.9(4); N3–Cd1–O1, 145.2(4); N3–Cd1–O2, 95.3(4); N3–Cd1–O4, 82.3(4); O1–Cd1–O2, 114.0(4); O1–Cd1–O4, 87.5(4); O2–Cd1–O4, 74.9(3); N4–Cd2–N5, 80.0(4); N4–Cd2–N6, 79.1(4); N4–Cd2–O2, 130.5(4); N4–Cd2–O3, 78.0(4); N4–Cd2–O4, 153.0(4); N5–Cd2–N6, 120.8(4); N5–Cd2–O2, 146.5(4); N5–Cd2–O3, 87.7(4); N5–Cd2–O4, 80.0(4); N6–Cd2–O2, 83.3(4); N6–Cd2–O3, 139.2(4); N6–Cd2–O4, 95.9(4); O2–Cd2–O3, 86.4(4); O2–Cd2–O4, 74.2(3); O3–Cd2–O4, 118.9(3); Cd1–O2–Cd2, 105.6(4); Cd1–O4–Cd2, 105.3(4).

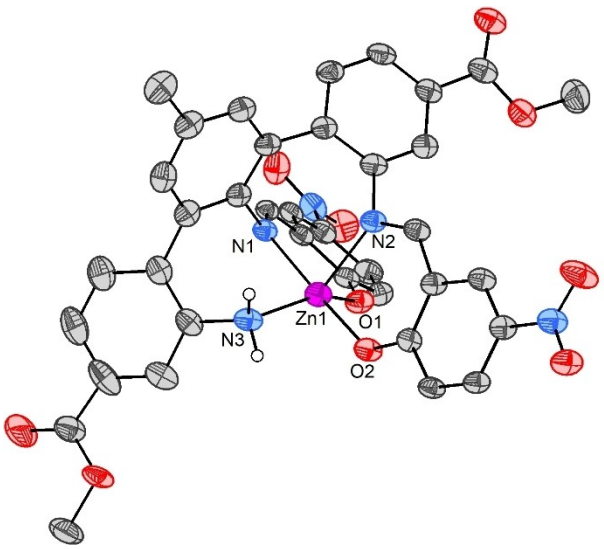

Figure 19. ORTEP plot of **1b-Zn–NH_2** with 50% probability ellipsoids. Hydrogen atoms (except for NH_2) and disorder in the one of the methoxycarbonyl substituents have been omitted for clarity. $\tau_5 = 0.33$. Selected bond lengths [Å] and angles [°]: Zn1–N1, 2.050(2); Zn1–N2, 2.205(2); Zn1–N3, 2.177(2); Zn1–O1, 1.9896(12); Zn1–O2, 1.9833(17); N1–Zn1–N2, 85.00(8); N1–Zn1–N3, 89.18(8); N1–Zn1–O1, 90.91(8); N1–Zn1–O2, 170.51(8); N2–Zn1–N3, 114.97(8); N2–Zn1–O1, 93.93(8); N2–Zn1–O2, 89.55(7); N3–Zn1–O1, 150.98(8); N3–Zn1–O2, 86.08(8); O1–Zn1–O2, 97.22(7).

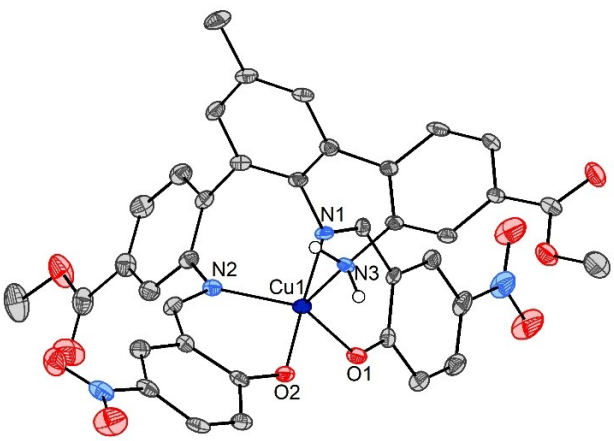

Figure 21. ORTEP plot of **1b-Cu–NH_2** with 50% probability ellipsoids. Hydrogen atoms (except for NH_2) have been omitted for clarity. $\tau_5 = 0.70$. Selected bond lengths [Å] and angles [°]: Cu1–N1, 1.933(3); Cu1–N2, 2.041(3); Cu1–N3, 2.299(3); Cu1–O1, 1.986(2); Cu1–O2, 1.903(2); N1–Cu1–N2, 91.95(11); N1–Cu1–N3, 86.83(11); N1–Cu1–O1, 92.02(11); N1–Cu1–O2, 172.46(12); N2–Cu1–N3, 114.29(11); N2–Cu1–O1, 130.68(11); N2–Cu1–O2, 91.23(11); N3–Cu1–O1, 115.00(10); N3–Cu1–O2, 85.64(10); O1–Cu1–O2, 91.08(10).

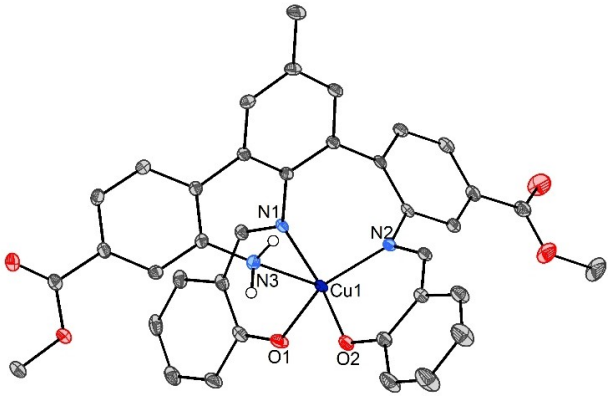

Figure 22. ORTEP plot of **1a-Cu**–NH_2 with 50% probability ellipsoids. Hydrogen atoms (except for NH_2) and non-coordinated EtOH (solvent of crystallization) have been omitted for clarity. $\tau_5 = 0.25$. Selected bond lengths [Å] and angles [°]: Cu1–N1, 1.9618(15); Cu1–N2, 1.9818(14); Cu1–N3, 2.4795(15); Cu1–O1, 1.9154(13); Cu1–O2, 1.9205(13); N1–Cu1–N2, 94.41(6); N1–Cu1–N3, 77.57(6); N1–Cu1–O1, 94.51(6); N1–Cu1–O2, 165.87(6); N2–Cu1–N3, 112.16(6); N2–Cu1–O1, 150.95(6); N2–Cu1–O2, 91.85(6); N3–Cu1–O1, 96.75(6); N3–Cu1–O2, 88.34(6); O1–Cu1–O2, 86.03(6).

On comparison of **1b-Zn**–NH_2 and **1b-Cu**–NH_2, a significantly longer metal-NH_2 bond was found for **1b-Cu**–NH_2 (Cu1–N3, 2.299(3) Å) than for **1b-Zn**–NH_2 (Zn1–N3, 2.177(2) Å). This may be attributed to weaker axial ligation for the d^9 Cu(II) center, compared to the d^{10} Zn(II) center.[46] This observation is consistent with literature reports, comparing Cu(II) complexes of pentadentate N_3O_2 ligands derived from bis(3-aminopopyl) amines and salicylaldehyde derivatives with their Zn(II) homologues.[41a,47] The elongated Cu–NH_2 bond found in **1b-Cu**–NH_2 is also in agreement with general observations concerning the bond lengths in crystal structures of pentacoordinated Cu(II) complexes, where one of the Cu-ligand bonds often is significantly longer than the others.[48] Comparing the nitro-substituted complex **1b-Cu**–NH_2 with its unsubstituted analog **1a-Cu**–NH_2, the large influence of the relatively peripheral nitro groups became evident. Nitro-substituted **1b-Cu**–NH_2 crystallized with distorted trigonal bipyramidal geometry, while **1a-Cu**–NH_2 crystallized with distorted square pyramidal geometry. The Cu–NH_2 bond was significantly longer for **1a-Cu**–NH_2 (Cu1–N3, 2.4795(15) Å) than for **1b-Cu**–NH_2 (Cu1–N3, 2.299(3) Å). Furthermore, the two other Cu–N bonds and the two Cu–O bonds were closer to each other in values for **1a-Cu**–NH_2 than for **1b-Cu**–NH_2.

Exploring 1d as a hexadentate ligand: Synthesis, single-crystal X-ray diffraction analysis and NMR studies of 1d-Lu

From the studies of Co(III) complexes **1a-Co(acac)** and **1d-Co(acac)**, it was observed that in case of rather small Co(III), potentially hexadentate ligands **1a** and **1d** would act as tetradentate $N_2O_2^{2-}$ ligands, leaving the third salicylaldimine group uncoordinated. From the NMR studies of Zn complexes **1a-Zn** and **1d-Zn**, however, there were indications that the imine nitrogen of the third salicylaldimine group could participate in coordination to the metal center, hence **1a** and **1d** would partially function as pentadentate $N_3O_2^{2-}$ ligands. To investigate whether e.g. **1d** could act as a hexadentate $N_3O_3^{3-}$ ligand, its reactivity towards Lu(III) was studied. The metal was chosen on basis of being trivalent and relatively large,[49] thus facilitating high coordination numbers as well as flexible coordination geometries,[50] which may be needed in order to accommodate ligand **1d**. In addition, Lu(III) possess the d^0 configuration, which renders the metal diamagnetic and suitable for conventional NMR studies, comparable to those of e.g. ligand **1d** and Zn complex **1d-Zn**. Reacting **1d** with $Lu(NO_3)_3 \cdot xH_2O$ lead to the successful formation of complex **1d-Lu** (Scheme 14).

Complex **1d-Lu** was characterized by NMR, MS, elemental analysis and single-crystal X-ray diffraction analysis. Combined ^1H, ^{13}C and ^{15}N NMR studies in different solvents suggested that **1d** coordinated in a hexadentate fashion to Lu, acting as an $N_3O_3^{3-}$ ligand.[51] This was most evident in the ^1H NMR spectrum of the complex, as no resonances that could be attributed to naphtholic protons were observed. Furthermore, imine coordination to Lu was rationalized from ^1H-^{15}N HMBC experiments, where small coordination shifts ($\Delta\delta(N^1) = 18.0$ ppm, and $\Delta\delta(N^2) = 2.8$ ppm, see Figure 27 for numbering scheme) were found for the imine nitrogen atoms in [D_6]DMSO. As opposed to what is commonly observed for coordination of metals to nitrogen atoms in ^{15}N NMR, the resonances corresponding to imine nitrogen atoms of **1d-Lu** were moved to higher ppm values on comparison with those of **1d**, indicating a rather weak interaction.[27b] Crystals suitable for single-crystal X-ray diffraction analysis of the complex were obtained from a DMSO/EtOH mixture, and it was found that the complex crystallized as the heptacoordinated complex **1d-Lu**–**DMSO** (Figure 23). A related heptacoordinated complex **1d-Lu**–**MeOH** (Figure 24) was obtained from recrystallization of **1d-Lu** from a $CDCl_3$/MeOH mixture.

Both Lu complexes crystallized with geometries best described as intermediate between capped octahedral and pentagonal bipyramidal. The bond lengths between Lu and the heteroatoms within the hexadentate ligand were similar for both complexes, with Lu–N and Lu–O bond lengths in the range of 2.350(3)–2.472(3) Å and 2.178(3)–2.200(3) Å respectively for **1d-Lu**–**DMSO**, and 2.362(16)–2.486(16) Å and 2.146(15)–2.193(13) Å respectively for **1d-Lu**–**MeOH**. In addition, the bond lengths were similar to what has been reported

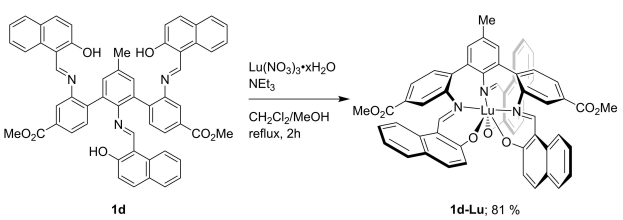

Scheme 14. Synthesis of **1d-Lu**. The product is depicted as a hexacoordinated complex for simplicity, although the complex is probably heptacoordinated, bearing an additional water ligand.

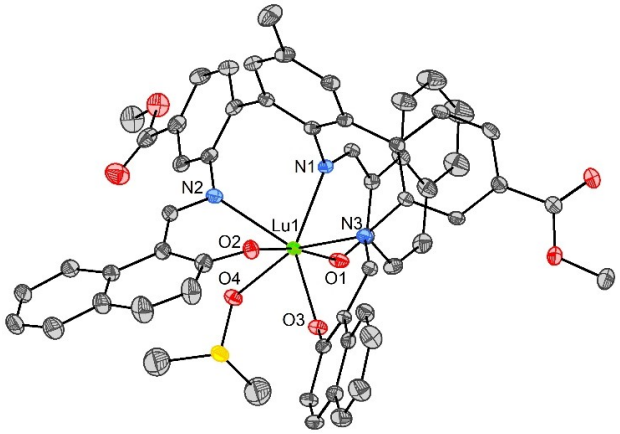

Figure 23. ORTEP plot of **1d-Lu**–**DMSO** with 50% probability ellipsoids. Hydrogen atoms and two non-coordinated molecules of DMSO (solvent of crystallization) have been omitted for clarity. Selected bond lengths [Å] and angles [°]: Lu1–N1, 2.350(3); Lu1–N2, 2.472(3); Lu1–N3, 2.445(3); Lu1–O1, 2.178(3); Lu1–O2, 2.200(3); Lu1–O3, 2.193(3); Lu1–O4, 2.268(3); N1–Lu1–N2, 76.50(10); N1–Lu1–N3, 78.42(10); N1–Lu1–O1, 73.61(10); N1–Lu1–O2, 114.68(10); N1–Lu1–O3, 143.30(10); N1–Lu1–O4, 127.83(10); N2–Lu1–N3, 128.00(10); N2–Lu1–O1, 115.15(10); N2–Lu1–O2, 71.61(10); N2–Lu1–O3, 140.17(10); N2–Lu1–O4, 71.33(10); N3–Lu1–O1, 100.00(10); N3–Lu1–O2, 78.91(10); N3–Lu1–O3, 74.90(10); N3–Lu1–O4, 153.02(10); O1–Lu1–O2, 170.95(10); O1–Lu1–O3, 86.65(10); O1–Lu1–O4, 84.24(10); O2–Lu1–O3, 84.39(10); O2–Lu1–O4, 92.74(10); O3–Lu1–O4, 78.80(10).

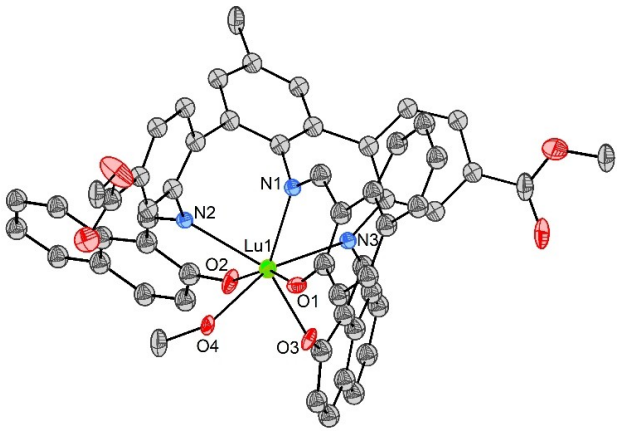

Figure 24. ORTEP plot of **1d-Lu**–**MeOH** with 50% probability ellipsoids. Hydrogen atoms have been omitted for clarity. The OH proton of the MeOH ligand could not be detected in the crystal structure. Selected bond lengths [Å] and angles [°]: Lu1–N1, 2.362(16); Lu1–N2, 2.477(17); Lu1–N3, 2.486(16); Lu1–O1, 2.165(14); Lu1–O2, 2.146(15); Lu1–O3, 2.193(13); Lu1–O4, 2.296(14); N1–Lu1–N2, 77.8(6); N1–Lu1–N3, 72.1(5); N1–Lu1–O1, 74.7(5); N1–Lu1–O2, 126.0(6); N1–Lu1–O3, 135.0(6); N1–Lu1–O4, 126.7(6); N2–Lu1–N3, 124.5(5); N2–Lu1–O1, 113.7(5); N2–Lu1–O2, 71.6(5); N2–Lu1–O3, 146.5(5); N2–Lu1–O4, 75.1(5); N3–Lu1–O1, 101.8(5); N3–Lu1–O2, 90.1(6); N3–Lu1–O3, 72.3(5); N3–Lu1–O4, 157.8(5); O1–Lu1–O2, 158.9(5); O1–Lu1–O3, 86.7(5); O1–Lu1–O4, 75.7(5); O2–Lu1–O3, 80.4(5); O2–Lu1–O4, 86.7(6); O3–Lu1–O4, 85.5(5).

in the literature for Lu–N and Lu–O bond lengths in Schiff base complexes of heptacoordinated Lu.[10g,52] The Lu–O(solvent) bond distances are in accordance with literature values for Lu–O(DMSO) and Lu–O(MeOH) bond lengths.[53]

The ^{1}H NMR spectrum of **1d-Lu** was found to be highly solvent-dependent. At ambient temperature in [D_6]DMSO and [D_7]DMF, the ^{1}H NMR resonances of each of the two methoxycarbonyl-substituted moieties in the complex were time-averaged (ring systems A′ in Figure 25), and the resonances of ring systems A′ and A integrated in a 2:1 ratio. Several of the ^{1}H and ^{13}C NMR resonances were broadened in [D_6]DMSO at ambient temperature, most notably the resonance corresponding to H$^{e'}$ (Figure 25). A gradual sharpening of the broadened resonances in the ^{1}H NMR spectrum of **1d-Lu** was observed on elevated temperatures in [D_6]DMSO (Figure 25).

The very broadened nature of the resonance corresponding to H$^{e'}$ at ambient temperature indicated dynamic behavior of the complex in [D_6]DMSO. For low-temperature ^{1}H NMR studies, [D_7]DMF was used, in which the complex had a similar ^{1}H NMR spectrum to that in [D_6]DMSO at ambient temperature. The ^{1}H NMR spectra of **1d-Lu** in the temperature range between 27 °C and −53 °C are shown in Figure 26.

On decreasing the temperature, the resonance corresponding to H$^{e'}$ gradually decoalesced into two new resonances (H$^{e'1}$ and H$^{e'2}$) (see Figure 26). Notably, a relatively large separation in chemical shifts for the resonances corresponding to H$^{e'1}$ and H$^{e'2}$ (δ 5.26 and δ 6.89) was observed, indicating that one of the methoxycarbonyl-substituted ring systems (A′ in Figure 26) must be significantly more shielded than the other. Because of the dynamic behavior of **1d-Lu** in [D_6]DMSO and [D_7]DMF, attention was turned to the coordination number of the complex in solution. Whereas ligand **1d** itself is hexadentate, Lu complexes usually possess coordination numbers of seven, eight or nine.[50,54] As both [D_6]DMSO and [D_7]DMF are strongly coordinating solvents, it is reasonable to assume that at least one solvent molecule is ligated to the Lu center in both solvents, as it is commonly seen in the coordination chemistry of rare earth metals.[55] In addition, solvent-ligation was already

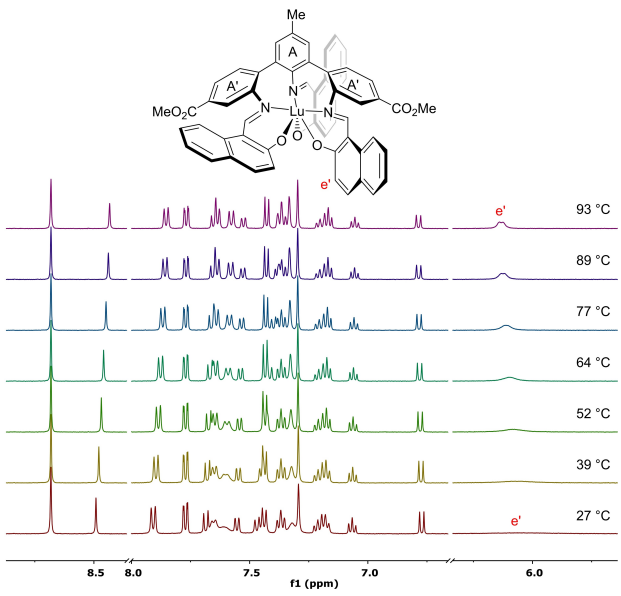

Figure 25. ^{1}H NMR of **1d-Lu** (500 MHz, [D_6]DMSO) at increasing temperatures (bottom to top). Only selected regions of the ^{1}H NMR spectra are shown.

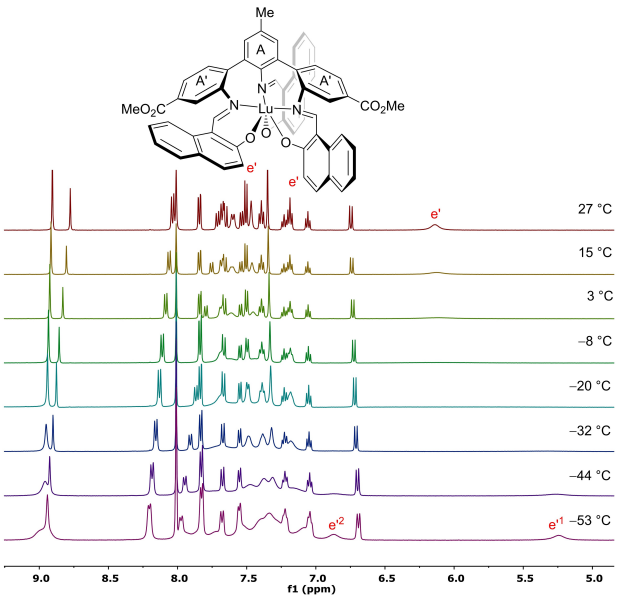

Figure 26. ^{1}H NMR of **1d**-**Lu** (500 MHz, [D_7]DMF) at increasing temperatures (bottom to top). Only the region between δ 5.0 and 9.25 is shown.

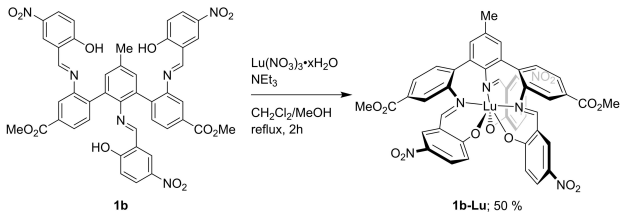

Scheme 15. Synthesis of **1b**-**Lu**. The product is depicted as a hexacoordinated complex for simplicity.

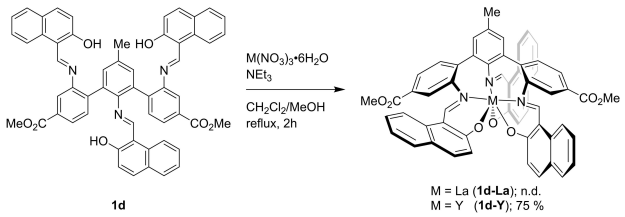

Scheme 16. Reactivity of ligand **1d** towards $La(NO_3)_3 \cdot 6H_2O$ and $Y(NO_3)_3 \cdot 6H_2O$.

observed from the crystallographic characterization of **1d**-**Lu**–**DMSO** and **1d**-**Lu**–**MeOH** (*vide supra*). Hepta-, octa- and nonacoordinated metal complexes are known to be stereochemically non-rigid,[56] which rationalize the dynamic behavior of **1d**-**Lu** in [D_6]DMSO and [D_7]DMF.[57] The combined structural and NMR-based investigations suggest that **1d**-**Lu** contains (at least) one labile monodentate ligand, which in combination with the high relative Lewis acidity of Lu(III),[58] makes it an interesting candidate for various applications, e.g. as a polymerization catalyst.[59] As **1d** acts a hexadentate $N_3O_3^{3-}$ ligand, the formation of monomeric complexes of Lu(III), as well as other rare earth metals (*vide infra*), should be favored compared to tetradentate $N_2O_2^{2-}$ salen-type ligands,[60] which occasionally give rise to dimeric complexes with rare earth metals,[59c] or homoleptic ML_2- or M_2L_3-type complexes.[10h,s,59b] However, it should be noted that dimer formation for rare earth metal complexes of e.g. heptadentate Schiff base ligands has been reported in the literature.[61]

As the nitro-substituted ligand **1b** was found to react in a different manner with $Zn(OAc)_2 \cdot 2H_2O$ than e.g. **1d**, the reactivity of **1b** towards $Lu(NO_3)_3 \cdot xH_2O$ was studied. Although a pure product could not be obtained, the ^{1}H NMR spectrum of the obtained product indicates that the ligand acts as an $N_3O_3^{3-}$ ligand towards Lu(III) (Scheme 15). This result shows again that the reactivity of ligand **1b** is highly metal-dependent, as already observed for Cu(II), Zn(II) and Cd(II).

A preliminary investigation of the reactivity of ligand **1d** towards larger rare-earth metals (Y(III) and La(III)) (Scheme 16) did not yield any fully conclusive results.

Complex **1d**-**Y** was obtained in good yields, and was characterized by NMR, as well as elemental analysis of its DMSO-ligated adduct **1d**-**Y**–**DMSO**. The complex was found to undergo demetallation during MS measurements, and attempts to obtain crystals for single-crystal X-ray diffraction analysis lead to crystal formation of the demetallated species, **1d** (which accordingly *could* be characterized by single-crystal X-ray diffraction analysis, *vide supra*). The ^{1}H NMR spectra of **1d**-**Y** in [D_6]DMSO and $CDCl_3$ were very similar to those of **1d**-**Lu**. Hence they will not be discussed in detail, but it should be noted that the ^{1}H NMR and ^{13}C NMR resonances of the Y(III) complex were less broadened than those of the Lu(III) complex in [D_6]DMSO at ambient temperature, while the opposite was observed in $CDCl_3$ (see Figure S256–S258, SI). The attempted synthesis of **1d**-**La** did not yield a clear outcome, and a complex mixture of different species was obtained instead (see Figure S259, SI). The unsuccessful attempt of synthesizing **1d**-**La** might be attributed to the considerably larger size of La(III) compared to Y(III) and Lu(III),[49] and issues concerning the successful coordination of early lanthanoids, the middle lanthanoids (having similar ionic radii as Y(III)) and the late lanthanoids to the same ligand system are occasionally reported in the literature.[62] The use of more reactive starting materials (e.g. the corresponding rare-earth bis(trimethylsilyl)amide compounds[63]) would perhaps lead to the successful synthesis of complexes of **1d** with the early lanthanoids, and this topic deserves further investigations.

Conclusion

Herein, the reactivity of new polydentate Schiff base ligands towards different metals was presented. For the reactions of $Zn(OAc)_2 \cdot 2H_2O$ and Schiff bases derived from a substituted 2,6,2′-triaminobiphenyl or a linear 2,2′,2″-triamino-*p*-terphenyl, the obtained complexes were similar to those Zn complexes that are commonly obtained from Schiff bases derived from 2,2′-diaminobiphenyl. For the reactions of $Zn(OAc)_2 \cdot 2H_2O$ and the hexadentate Schiff bases derived from a substituted 2,2′,2″-

triamino-*m*-terphenyl and either salicylaldehyde or 2-hydroxy-1-naphthaldehyde, the obtained complexes were found to exist as either tetracoordinated monomeric complexes, or pentacoordinated monomeric or dimeric/oligomeric species in solution, as observed by NMR spectroscopy. For a related hexadentate ligand obtained from the condensation of the same 2,2′,2″-triamino-*m*-terphenyl and 5-nitrosalicylaldehyde, a pentadentate, NH_2-containing ligand was formed upon reaction with $Zn(OAc)_2 \cdot 2H_2O$ and $Cd(OAc)_2 \cdot 2H_2O$, and complexes containing a labile metal-NH_2 bond were isolated as the sole products. When the same reaction was carried out using $Cu(OAc)_2 \cdot H_2O$, a mixture of different products were obtained instead, most notably an NH_2-containing pentacoordinated complex as well as a tetracoordinated complex, analogous to those that were obtained for Zn using ligands derived from less electron poor salicylaldehydes. The pentacoordinated complex could be synthesized selectively by reacting the 2,2′,2″-triamino-*m*-terphenyl with 2 equivalents of 5-nitrosalicylaldehyde in the presence of $Cu(OAc)_2 \cdot H_2O$. The method was successfully extended to salicylaldehyde, yielding another pentacoordinated Cu complex. Finally, one of the *m*-terphenyl ligands that acted as tetradentate/pentadentate ligand towards divalent and relatively small Zn(II), was found to act as a hexadentate ligand towards larger and trivalent Lu(III) and Y(III). The results presented herein highlight the versatility of the triamine-*m*-terphenyl backbone and its Schiff base ligands, creating metal complexes with easily tunable properties. Further studies should focus on the application of the complexes in various catalytic settings, as well as broadening the scope of the synthesis of rare earth metal complexes.

Experimental Section

Triamines **5**–**7**,[17] and Schiff base ligands **8**–**9**[14] were synthesized as described elsewhere. THF (unstabilized), MeCN and CH_2Cl_2 were dried using an MB SPS-800 solvent purifier system from MBraun. Toluene was dried using 3 Å molecular sieves. Hexanes and ethyl acetate were distilled before use. Other chemicals and solvents were used as received from commercial sources. TLC was performed using Merck 60 F254 plates. Flash chromatography was performed using silica gel from Merck (60, 0.040–0.063 mm). NMR spectroscopy was performed using Bruker Avance DPX300, AVII400, AVIIIHD400, DRX500, AVI600, AVII600 or AVIIHD800 operating at 300 MHz (^{1}H NMR), or 400 MHz (^{1}H NMR), 376 MHz (^{19}F NMR), 101 MHz (^{13}C NMR), or 500 MHz (^{1}H NMR), or 600 MHz (^{1}H NMR) and 151 MHz (^{13}C NMR), or 800 MHz (^{1}H NMR) and 201 MHz (^{13}C NMR) respectively. All spectra were recorded at room temperature unless otherwise mentioned. The temperature of the variable temperature NMR experiments was measured indirectly by correlation of the observed probe temperature to independently measured temperatures (or extrapolated temperatures for the temperatures above the boiling point of methanol) using a Delta OHM HD9214 thermometer fitted into a NMR tube containing CD_3OD/CH_3OH. Because of this, small deviations in the exact temperature cannot be excluded. ^{1}H NMR and ^{13}C NMR spectra have been referenced relative to the residual solvent signals, and the peaks are numbered according to Figure 27. Chemical shifts in ^{19}F NMR have been referenced to $CFCl_3$ by using C_6F_6 (−164.9 ppm with respect to $CFCl_3$ at 0 ppm) as an internal standard, and are proton decoupled. Chemical shifts in ^{15}N NMR have been calibrated against CH_3NO_2 as an external standard (0.0 ppm). All ^{15}N NMR chemical shifts were obtained and assigned using ^{1}H–^{15}N HMBC experiments. The peaks in the ^{1}H NMR and ^{13}C NMR spectra were assigned using various 2D experiments (NOESY, COSY, TOCSY, HSQC, HMBC and HETCOR). MS (ESI) was recorded on a Bruker maXis II ETD spectrometer. All melting points are uncorrected and were obtained with a Stuart SMP10 melting point apparatus. UV/Vis measurements were performed on a Specord 200 Plus instrument. Elemental analysis was performed by Mikroanalytisches Laboratorium Kolbe, Oberhausen, Germany. Single-crystal diffraction data were acquired on a Bruker D8 Venture equipped with a Photon 100 CMOS area detector, and using Mo Kα radiation (λ = 0.71073 Å) from an Incoatec iμS microsource. Data reduction was performed with the Bruker Apex3 Suite, the structures were solved with ShelXT[64] and refined with ShelXL.[65] Olex2 was used as user interface.[66] The cif files were edited with enCIFer v. 1.4.[67] Disordered solvent molecules in the structures of **1a-Zn**, **1b-Zn**–NH_2, **1b-Cu**–NH_2 and **1d-Lu**–**MeOH** were removed using the SQUEEZE algorithm.[68] Molecular graphics were produced with Diamond v. 4.6.2. Full details of the data collection, structure solution and refinement for each compound are contained in the cif files. The data are summarized in Table S1–Table S15, SI.

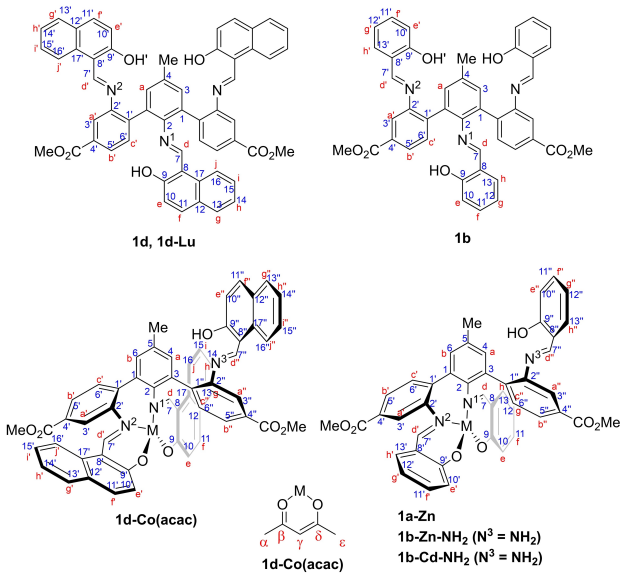

Figure 27. Numbering scheme used for reporting the NMR data. Roman letters = protons, numbers = carbons. Greek letters = protons and carbons. For **1b-Zn**–NH_2 and **1b-Cd**–NH_2, imine nitrogen N^3 is not present, instead an NH_2 group is present. For complex **1b-Cd**, the imine nitrogen N^3 is present, although this species was only observed in MS.

Experimental and analytical data for a selection of compounds described within the text are presented here, data for all compounds can be found in the SI.

1b. A suspension of triamine **5** (0.408 g, 1.01 mmol, 1.0 equiv.), 5-nitrosalicylaldehyde (0.555 g, 3.31 mmol, 3.3 equiv.) and HCO_2H (10 drops) in EtOH (10 mL) was heated at reflux temperature for 3 days. After cooling to rt, the precipitated solids were filtered off, and washed with EtOH. **1b** was obtained as orange crystals after recrystallization from MeCN. Yield: 0.656 g, 0.770 mmol, 76%. M.p. 170–172 °C; ^{1}H NMR (800 MHz, $CDCl_3$, major rotamer): δ = 13.30 (s, 2H, OH′), 12.78 (s, 1H, OH), 8.53 (s, 2H, $H^{d'}$), 8.25 (d, $^3J_{H,H}$ = 9.1 Hz, 2H, H^{f}), 8.19 (s, 2H, $H^{h'}$), 8.11 (d, $^3J_{H,H}$ = 7.8 Hz, 2H, $H^{b'}$), 8.04 (m, 1H, H^{f}), 7.88 (s, 2H, $H^{a'}$), 7.71–7.72 (m, 3H, H^{d} + $H^{c'}$), 7.40 (s, 1H, H^{h}), 7.27 (s, 2H, H^{a}), 7.03 (d, $^3J_{H,H}$ = 9.1 Hz, 2H, $H^{e'}$), 6.71 (d, $^3J_{H,H}$ = 9.1 Hz, 1H, H^{e}),

3.95 (s, 6H, CO_2CH_3), 2.49 ppm (s, 3H, Ar–CH_3); ^{13}C NMR (201 MHz, $CDCl_3$, major rotamer): δ = 165.9 ($C^{9'}$), 165.8 (CO_2CH_3), 165.6 (C^9), 164.6 (C^7), 161.3 ($C^{7'}$), 144.8 ($C^{2'}$), 141.9 (C^2), 140.2 ($C^{12'}$), 139.8 (C^{12}), 139.4 ($C^{1'}$), 137.3 (C^4), 131.9 (C^3), 131.5 ($C^{6'}$), 131.4 (C^1), 131.2 ($C^{4'}$), 129.2 ($C^{5'}$), 128.8 ($C^{11'}$), 128.6 (C^{11}), 128.5 ($C^{13'}$), 127.6 (C^{13}), 118.8 ($C^{3'}$), 118.1 ($C^{10}+C^{10'}$), 118.0 ($C^{8'}$), 117.1 (C^8), 52.5 (CO_2CH_3), 21.1 ppm (Ar–CH_3); ^{15}N{^{1}H} NMR (600 MHz, $CDCl_3$): δ = −13.2 (NO_2), −85.6 ppm (CH=N^1 + CH=N^2); LRMS (ESI): *m/z* (%): 875.191 (100) [*M* + Na]$^+$; HRMS (ESI): *m/z* calcd for $C_{44}H_{32}N_6O_{13}$ + Na: 875.1920 [*M* + Na]$^+$; found: 875.1921; elemental analysis calcd (%) for $C_{44}H_{32}N_6O_{13}$: C 61.97, H 3.78, N 9.86; found: C 62.02, H 3.76, N 9.83.

For ^{1}H NMR and ^{13}C NMR data of the minor rotamer of **1b** in $CDCl_3$, see SI. Additional NMR data in C_6D_6 are also presented in the SI.

1d. A suspension of triamine **5** (0.412 g, 1.02 mmol, 1.0 equiv.), 2-hydroxy-1-naphthaldehyde (0.582 g, 3.38 mmol, 3.3 equiv.) and HCO_2H (10 drops) in EtOH (10 mL) was heated at reflux temperature for 2 days. After cooling to rt, the precipitated solids were filtered off, and washed with EtOH. **1d** was obtained as golden yellow crystals after recrystallization from 10% benzene in MeCN. Yield: 0.708 g, 0.815 mmol, 80%. M.p. 266–267 °C; ^{1}H NMR (600 MHz, [D_6]DMSO, major rotamer): δ = 14.73 (s, 2H, OH′), 13.63 (s, 1H, OH), 9.28 (s, 2H, $H^{d'}$), 8.50 (s, 1H, H^d), 8.08–8.13 (m, 4H, $H^{a'}+H^{i'}$), 7.97 (d, $^3J_{H,H}$ = 7.9 Hz, 2H, $H^{b'}$), 7.86 (d, $^3J_{H,H}$ = 9.1 Hz, 2H, $H^{f'}$), 7.80 (d, $^3J_{H,H}$ = 7.9 Hz, 2H, $H^{c'}$), 7.68 (d, $^3J_{H,H}$ = 7.9 Hz, 2H, $H^{g'}$), 7.57 (d, $^3J_{H,H}$ = 9.0 Hz, 1H, H^f), 7.45 (d, $^3J_{H,H}$ = 8.0 Hz, 1H, H^g), 7.39 (s, 2H, H^a), 7.30–7.33 (m, 2H, $H^{i'}$), 7.23–7.26 (m, 2H, $H^{h'}$), 6.98–7.02 (m, 3H, $H^h+H^{e'}$), 6.82–6.84 (m, 1H, H^i), 6.59 (d, $^3J_{H,H}$ = 8.5 Hz, 1H, H^j), 6.55 (d, $^3J_{H,H}$ = 9.0 Hz, 1H, H^e), 3.83 (s, 6H, CO_2CH_3), 2.48 ppm (s, 3H, Ar–CH_3); ^{13}C NMR (151 MHz, [D_6]DMSO, major rotamer): δ = 167.2 ($C^{9'}$), 165.7 (CO_2CH_3), 163.1 (C^9), 161.5 (C^7), 157.6 ($C^{7'}$), 144.1 ($C^{2'}$), 142.8 (C^2), 138.3 ($C^{1'}$), 136.5 ($C^{11'}$), 135.7 (C^4), 135.2 (C^{11}), 132.6 ($C^{17'}$), 131.6 (C^{17}), 131.5 ($C^{6'}$), 131.3 (C^3), 131.2 (C^1), 130.5 ($C^{4'}$), 128.7 ($C^{13'}$), 128.5 (C^{13}), 127.7 ($C^{15'}$), 127.2 (C^{15}), 126.9 ($C^{5'}$), 126.8 ($C^{12'}$), 126.6 (C^{12}), 123.4 ($C^{14'}$), 123.0 (C^{14}), 120.7 ($C^{10'}$), 120.4 ($C^{16'}$), 119.2 (C^{10}), 119.1 ($C^{3'}$), 117.8 (C^{16}), 109.1 ($C^{8'}$), 107.8 (C^8), 52.3 (CO_2CH_3), 20.5 ppm (Ar–CH_3); ^{15}N{^{1}H} NMR (600 MHz, [D_6] DMSO): δ = −115.0 ppm (CH=N^2), −136.0 ppm (CH=N^1); LRMS (ESI): *m/z* (%): 890.284 (100) [*M* + Na]$^+$; HRMS (ESI): *m/z* calcd for $C_{56}H_{41}N_3O_7$ + Na: 890.2837 [*M* + Na]$^+$; found: 890.2841; elemental analysis calcd (%) for $C_{56}H_{41}N_3O_7$: C 77.49, H 4.76, N 4.84; found: C 77.48, H 4.76, N 4.83.

For ^{1}H NMR and ^{13}C NMR data of the minor rotamer of **1d** in [D_6] DMSO, see SI. Additional NMR data in different solvents and at different temperatures are also presented in the SI. Crystals of **1d** suitable for single-crystal X-ray diffraction analysis were obtained from vapor diffusion of EtOH into a DMSO solution of the Y complex **1d**-**Y**. Crystal and refinement data are given in Table S1, SI.

1a-**Zn**. Ligand **1a** (0.356 g, 0.495 mmol, 1.0 equiv.) was dissolved in CH_2Cl_2 (2 mL). NEt_3 (0.35 mL, 2.5 mmol, 5.0 equiv.) was added, followed by a solution of $Zn(OAc)_2\cdot 2H_2O$ (0.113 g, 0.513 mmol, 1.0 equiv.) in MeOH (10 mL). A solid started to precipitate within few minutes, and the resulting pale yellow suspension was stirred at rt for 18 h. The solids were then filtered off and washed with MeOH. **1a**-**Zn** was obtained as pale yellow crystals after recrystallization from MeCN. Yield: 0.277 g, 0.355 mmol, 72%. M.p. 213–215 °C; ^{1}H NMR (600 MHz, [D_6]DMSO): δ = 12.38 (s, 1H, OH), 9.00 (s, 1H, $H^{d''}$), 8.18 (s, 1H, $H^{d'}$), 7.93 (s, 1H, $H^{a''}$), 7.89 (dd, $^3J_{H,H}$ = 8.0 Hz, $^4J_{H,H}$ = 1.7 Hz, 1H, $H^{b'}$), 7.73 (s, 1H, $H^{h''}$), 7.71 (dd, $^3J_{H,H}$ = 8.0 Hz, $^4J_{H,H}$ = 1.6 Hz, 1H, $H^{b''}$), 7.63 (s, H^d), 7.59–7.60 (m, 2H, $H^{a'}+H^{c'}$), 7.51 (d, $^3J_{H,H}$ = 7.5 Hz, 1H, $H^{c''}$), 7.41 (s, 1H, $H^{f''}$), 7.21–7.24 (m, 2H, $H^f+H^{h'}$), 7.19 (s, 1H, H^a), 7.12 (s, 1H, H^b), 7.05 (ddd, $^3J_{H,H}$ = 8.5 Hz, $^3J_{H,H}$ = 6.8 Hz, $^4J_{H,H}$ = 1.6 Hz, 1H, H^f), 6.98 (s, 1H, $H^{g''}$), 6.93 (s, 1H, $H^{e''}$), 6.78 (d, $^3J_{H,H}$ = 6.8 Hz, 1H, $H^{e'}$), 6.54 (s, 1H, H^h), 6.44–6.46 (m, 2H, $H^e+H^{g'}$), 6.20 (s, 1H, H^g), 3.86 (s, 3H, $CO_2CH'_3$), 3.84 (s, 3H, $CO_2CH''_3$), 2.30 ppm (s, 3H, Ar–CH_3); ^{13}C NMR (201 MHz, [D_6]DMSO): δ = 173.0 (C^7), 171.3 ($C^{9'}$), 171.1 (C^9), 168.4 ($C^{7'}$), 165.6 ($C'O_2CH_3$), 165.5 ($C''O_2CH_3$), 164.3 ($C^{7''}$), 160.1 ($C^{9''}$), 148.1 ($C^{2'}$), 147.2 ($C^{2''}$), 144.1 (C^2), 138.7 ($C^{1''}$), 137.7 ($C^{1'}$), 136.2 ($C^{13'}$), 135.5 (C^{13}), 135.1 (C^5), 134.8 (C^{11}), 134.6 ($C^{11'}$), 133.6 ($C^{11''}$), 133.0 ($C^{13''}$), 132.7 (C^1 or C^3), 132.3 (C^4+C^1 or C^3), 132.0 ($C^{6''}$), 131.0 (C^6), 130.6 ($C^{6'}$), 129.9 ($C^{4''}$), 129.7 ($C^{4'}$), 126.8 ($C^{5''}$), 126.6 ($C^{5'}$), 123.2 ($C^{3'}$), 122.8 ($C^{10'}$), 122.2 (C^{10}), 119.4 ($C^{8''}$), 119.1 ($C^{8'}+C^{12''}$), 118.9 ($C^{3''}$), 117.8 (C^8), 116.5 ($C^{10''}$), 113.1 $C^{12'}$), 112.9 (C^{12}), 52.2 ($CO_2C'H_3$ or $CO_2C''H_3$), 52.1 ($CO_2C'H_3$ or $CO_2C''H_3$), 20.2 ppm (Ar–CH_3). Several of the ^{1}H and ^{13}C NMR resonances were broadened. ^{15}N{^{1}H} NMR (600 MHz, [D_6]DMSO): δ = −89.0 (CH=N^3), −123.4 (CH=N^2–Zn), −131.8 ppm (CH=N^1–Zn); LRMS (ESI): *m/z* (%): 802.150 (100) [*M* + Na]$^+$; HRMS (ESI): *m/z* calcd for $C_{44}H_{33}N_3O_7Zn$ + Na: 802.1502 [*M* + Na]$^+$; found: 802.1501; elemental analysis calcd (%) for $C_{44}H_{33}N_3O_7Zn$: C 67.66, H 4.26, N 5.38, Zn 8.37; found: C 67.48, H 4.24, N 5.35, Zn 8.32.

For additional NMR data for **1a**-**Zn** in different solvents and at different temperatures, see SI. Crystals of **1a**-**Zn** suitable for single-crystal X-ray diffraction analysis were obtained by slow evaporation of a solution of the complex in THF. Crystal and refinement data are given in Table S2, SI.

1b-**Zn**–$\mathbf{NH_2}$. Ligand **1b** (0.434 g, 0.508 mmol, 1.0 equiv.) was dissolved in CH_2Cl_2 (10 mL). NEt_3 (0.35 mL, 2.5 mmol, 4.9 equiv.) was added, and the originally yellow solution quickly turned red-brown. A solution of $Zn(OAc)_2\cdot 2H_2O$ (0.114 g, 0.522 mmol, 1.0 equiv.) in MeOH (10 mL) was then added, and a pale yellow precipitate formed within 30 min of stirring at rt. The resulting suspension was stirred for a total reaction time of 18 h at rt. Additional MeOH (10 mL) was added, and the reaction mixture was stirred for a few minutes before the product was filtered off and washed with MeOH, furnishing **1b**-**Zn**–$\mathbf{NH_2}$ as a pale yellow solid. Yield: 0.320 g, 0.418 mmol, 82%. M.p. > 310 °C; ^{1}H NMR (600 MHz, [D_6]DMSO): δ = 8.69 (s, 1H, $H^{d'}$), 8.51 (d, $^4J_{H,H}$ = 3.1 Hz, 1H, $H^{h'}$), 8.11 (dd, $^3J_{H,H}$ = 9.5 Hz, $^4J_{H,H}$ = 3.1 Hz, 1H, $H^{f'}$), 7.94–7.96 (m, 2H, $H^{a''}+H^{b'}$), 7.90–7.91 (m, 2H, H^d+H^h), 7.87 (dd, $^3J_{H,H}$ = 9.5 Hz, $^4J_{H,H}$ = 3.1 Hz, 1H, H^f), 7.67 (d, $^4J_{H,H}$ = 1.7 Hz, 1H, $H^{a'}$), 7.58–7.59 (m, 2H, $H^{b''}+H^{c'}$), 7.48 (d, $^3J_{H,H}$ = 7.9 Hz, 1H, $H^{c''}$), 7.37 (d, $^4J_{H,H}$ = 1.5 Hz, 1H, H^a), 7.34 (d, $^4J_{H,H}$ = 1.2 Hz, 1H, H^b), 6.79 (d, $^3J_{H,H}$ = 9.5 Hz, 1H, $H^{e'}$), 6.53 (d, $^3J_{H,H}$ = 9.5 Hz, 1H, H^e), 6.17 (broadened s, 2H, NH_2), 3.81 (s, 3H, $CO_2CH'_3$), 3.78 (s, 3H, $CO_2CH''_3$), 2.43 ppm (s, 3H, Ar–CH_3); ^{13}C NMR (151 MHz, [D_6]DMSO): δ = 176.1 ($C^{9'}$), 176.0 (C^9), 173.4 ($C^{7'}$), 168.7 (C^7), 165.8 ($C''O_2CH_3$), 165.3 ($C'O_2CH_3$), 149.0 ($C^{2'}$), 140.7 ($C^{2''}$), 140.6 (C^2), 136.8 ($C^{1'}$), 136.6 (C^5), 134.9 ($C^{13'}$), 134.3 ($C^{12'}$), 134.1 (C^{12}), 133.1 (C^{13}), 131.4 ($C^{6'}$), 131.0 ($C^4+C^{6''}$), 130.8 (C^3), 130.7 ($C^{4'}$), 130.6 ($C^{1''}$), 130.5 (C^3+C^6), 129.7 ($C^{4''}$), 129.1 ($C^{11'}$), 129.0 (C^{11}), 127.7 ($C^{5'}$), 124.9 ($C^{3'}$), 123.6 ($C^{10'}$), 123.4 (C^{10}), 123.0 ($C^{5''}$), 121.5 ($C^{3''}$), 118.3 ($C^{8''}$), 117.1 (C^8), 52.3 ($CO_2C'H_3$), 52.1 ($CO_2C''H_3$), 20.5 ppm (Ar–CH_3); ^{15}N{^{1}H} NMR (600 MHz, [D_6]DMSO): δ = −11.2 (2×NO_2), −120.9 (CH=N^2–Zn), −125.6 (CH=N^1–Zn), −326.9 ppm ($|^1J_{N,H}|$ = 72 Hz, NH_2); LRMS (ESI): *m/z* (%): 788.094 (100) [*M* + Na]$^+$; HRMS (ESI): *m/z* calcd for $C_{37}H_{27}N_5O_{10}Zn$ + Na: 788.0942 [*M* + Na]$^+$; found: 788.0945; elemental analysis calcd (%) for $C_{37}H_{27}N_5O_{10}Zn$: C 57.94, H 3.55, N 9.13, Zn 8.52; found: C 57.75, H 3.51, N 9.09, Zn 8.49.

For NMR data of the minor species of **1b**-**Zn**–$\mathbf{NH_2}$ in [D_6]DMSO (**1b**-**Zn**-**DMSO**), see SI. Additional NMR data in different solvents and at different temperatures are also presented in the SI. Crystals of **1b**-**Zn**–$\mathbf{NH_2}$ suitable for single-crystal X-ray diffraction analysis were obtained by performing the abovementioned procedure under more diluted conditions (CH_2Cl_2 (20 mL) and MeOH (20 mL) were used), and without any stirring, furnishing **1b**-**Zn**–$\mathbf{NH_2}$ as yellow crystals during the course of 1 day. The product obtained by this crystallization method had an identical ^{1}H NMR spectrum to the product obtained from the abovementioned method. Crystal and refinement data are given in Table S7, SI.

1b-Cd–NH$_2$. The Cd complex was prepared analogously to **1b-Zn–NH$_2$**, by employing **1b** (0.433 g, 0.508 mmol, 1.0 equiv.), Cd(OAc)$_2$·2H$_2$O (0.134 g, 0.505 mmol, 1.0 equiv.), NEt$_3$ (0.35 mL, 2.5 mmol, 4.9 equiv.), CH$_2$Cl$_2$ (10 mL) and MeOH (10 + 10 mL). **1b-Cd–NH$_2$** was obtained as a yellow solid. Yield: 0.325 g, 0.400 mmol, 79 %. M.p. > 310 °C; ^{1}H NMR (600 MHz, [D$_6$]DMSO): δ = 8.37–8.42 (m, 2H, H$^{d'}$ + H$^{h'}$), 7.96–7.98 (m, 1H, H^{f}), 7.83–7.85 (m, 1H, H$^{b'}$), 7.73–7.80 (m, 3H, H^{d} + H$^{f'}$ + H^{h}), 7.63 (s, 1H, H$^{a''}$), 7.51 (s, 1H, H$^{a'}$), 7.43–7.44 (m, 2H, H$^{c'}$ + H$^{b''}$), 7.31–7.34 (m, 1H, H$^{c''}$), 7.20 (s, 1H, H^{a}), 7.18 (s, 1H, H^{b}), 6.55–6.58 (m, 1H, H$^{e'}$), 6.32–6.34 (m, 1H, H^{e}), 5.27 (m, 2H, NH_2), 3.83 (s, 3H, CO$_2$CH'_3), 3.78 (s, 3H, CO$_2$CH''_3), 2.37 ppm (s, 3H, Ar–CH_3); ^{13}C NMR (151 MHz, [D$_6$]DMSO): δ = 177.8 (C$^{9'}$), 177.6 (C^{9}), 171.2 (C$^{7'}$), 170.9 (C^{7}), 166.2 (C$''$O$_2$CH$_3$), 165.6 (C$'$O$_2$CH$_3$), 150.5 (C$^{2'}$), 143.6 (C^{2}), 142.3 (C$^{2''}$), 137.4 (C$^{1'}$), 135.4 (C^{5} + C$^{13'}$), 134.1 (C^{13}), 133.0 (C$^{12'}$), 132.4 (C^{12}), 132.3 (C$^{1''}$), 131.8 (C^{1}), 131.0 (C$^{6'}$), 131.0 (C^{4}), 130.7 (C$^{6''}$), 130.3 (C^{6}), 130.2 (C^{3}), 130.1 (C$^{4'}$), 129.2 (C$^{4''}$), 128.09 (C^{11}), 128.02 (C$^{11'}$), 126.5 (C$^{5'}$), 124.14 (C$^{10'}$), 123.6 (C^{10}), 123.59 (C$^{3'}$), 120.8 (C$^{5''}$), 120.1 (C$^{3''}$), 119.3 (t, $^3J_{C,Cd}$ = 18.7 Hz, C$^{8'}$), 118.0 (t, $^3J_{C,Cd}$ = 22.3 Hz, C^{8}), 52.3 (CO$_2$C$'$H$_3$), 52.0 (CO$_2$C$''$H$_3$), 20.4 ppm (Ar–CH$_3$). Several of the ^{1}H and ^{13}C NMR resonances were broadened. ^{15}N{^{1}H} NMR (600 MHz, [D$_6$] DMSO): δ = −11.4 (2 × NO$_2$), −97.8 (CH=N^2–Cd), −112.6 (CH=N^1–Cd), −322.7 ppm (|$^1J_{N,H}$| = 77 Hz, NH$_2$); LRMS (ESI, positive mode): *m/z* (%): 838.069 (14) [*M* + Na]$^+$; HRMS (ESI): *m/z* calcd for C$_{37}$H$_{27}$^{110}CdN$_5$O$_{10}$ + Na: 834.0680 [*M* + Na]$^+$; found: 834.0677; LRMS (ESI, negative mode): *m/z* (%): 702.184 (< 10), 814.072 (29) [**1b-Cd–NH$_2$**–H]$^-$, 850.048 (100) [**1b-Cd–NH$_2$** + Cl]$^-$, 963.084 (< 10) [**1b-Cd**–H]$^-$; HRMS (ESI, negative mode): *m/z* calcd for C$_{37}$H$_{26}$^{110}CdN$_5$O$_{10}$: 810.0715 [**1b-Cd–NH$_2$**–H]$^-$; found: 810.0710; *m/z* calcd for C$_{37}$H$_{27}$^{110}CdN$_5$O$_{10}$ + Cl: 846.0482 [**1b-Cd–NH$_2$** + Cl]$^-$, found: 846.0475; *m/z* calcd for C$_{44}$H$_{29}$^{110}CdN$_6$O$_{13}$: 959.0828 [**1b-Cd**–H]$^-$, found: 959.0821; elemental analysis calcd (%) for C$_{37}$H$_{27}$N$_5$O$_{10}$Cd: C 54.59, H 3.34, N 8.60, Cd 13.81; found: C 54.41, H 3.27, N 8.55, Cd 13.76.

Complex **1b-Cd** was only observed by MS. For NMR data of the minor species of **1b-Cd–NH$_2$** in [D$_6$]DMSO (**1b-Cd–DMSO**), see SI. Additional NMR data in different solvents and at different temperatures are also presented in the SI. Crystals of **1b-Cd–NH$_2$** suitable for single-crystal X-ray diffraction analysis were obtained by slow diffusion of MeOH into a solution of the complex in DMSO. Alternatively, crystals could obtained by performing the above-mentioned procedure under more diluted conditions (CH$_2$Cl$_2$ (20 mL) and MeOH (20 mL) were used), and without any stirring, furnishing **1b-Cd–NH$_2$** as yellow crystals during the course of 1 day. The product obtained by this method had an identical ^{1}H NMR spectrum to the product obtained from the abovementioned method. Crystal and refinement data are given in Table S8, SI.

1b-Cu–NH$_2$. Triamine **5** (0.200 g, 0.493 mmol, 1.0 equiv.), Cu(OAc)$_2$·H$_2$O (0.098 g, 0.49 mmol, 1.0 equiv.) and 5-nitrosalicylaldehyde (0.165 mg, 0.987 mmol, 2.0 equiv.) were stirred in toluene (2 mL) overnight. The product was isolated by gravity filtration, washed with toluene (2 × 1 mL) and then dried in a vacuum oven at 70 °C over night, yielding the product as a bright green solid. Yield: 0.315 g, 0.412 mmol, 84 %. UV/Vis (CH$_2$Cl$_2$): λ$_{max}$ (ε) = 259 (62000), 365 (36000), 677 nm (327 mol^{-1}dm^{3}cm^{-3}); LRMS (ESI): *m/z* (%): 787.095 (100) [*M* + Na]$^+$; HRMS (ESI): *m/z* calcd for C$_{37}$H$_{27}$CuN$_5$O$_{10}$ + Na: 787.0946 [*M* + Na]$^+$; found: 787.0947; elemental analysis calcd (%) for C$_{37}$H$_{27}$CuN$_5$O$_{10}$: C 58.08, H 3.56, N 9.15, Cu 8.30; found: C 57.67, H 3.59, N 9.17, Cu 8.24.

Recrystallization by vapor diffusion of methanol into a solution of **1b-Cu–NH$_2$** in DMSO yielded crystals suitable for single-crystal X-ray diffraction analysis. Crystal and refinement data are given in Table S11, SI.

1d-Co(acac). Ligand **1d** (0.431 g, 0.496 mmol, 1.0 equiv.) and Co(acac)$_3$ (0.177 g, 0.496 mmol, 1.0 equiv.) were dissolved in toluene (10 mL), and the dark green-brown solution was heated at reflux temperature under Ar for 3 days. After cooling to rt, the reaction mixture was diluted with CH$_2$Cl$_2$ (50 mL), and evaporated to dryness under reduced pressure. Purification by flash chromatography (95 % CH$_2$Cl$_2$/5 % EtOAc), followed by recrystallization from MeCN/benzene (5:1) gave **1d-Co(acac)** as dark green crystals. Yield: 0.290 g, 0.283 mmol, 57 %. ^{1}H NMR (600 MHz, CDCl$_3$): δ = 14.53 (d, $^4J_{H,H}$ = 2.1 Hz, 1H, OH), 9.19 (d, $^4J_{H,H}$ = 2.1 Hz, 1H, H$^{d''}$), 8.10 (dd, $^3J_{H,H}$ = 8.1 Hz, $^4J_{H,H}$ = 1.6 Hz, 1H, H$^{b'}$), 8.02 (d, $^3J_{H,H}$ = 8.5 Hz, 1H, H$^{j''}$), 7.99 (s, 1H, H$^{d'}$), 7.97 (d, $^3J_{H,H}$ = 8.1 Hz, 1H, H$^{c''}$), 7.85–7.87 (m, 2H, H$^{b''}$ + H$^{f''}$), 7.76–7.78 (m, 2H, H$^{a'}$ + H$^{g''}$), 7.70 (d, $^3J_{H,H}$ = 8.5 Hz, 1H, H$^{j'}$), 7.68 (d, $^3J_{H,H}$ = 8.1 Hz, 1H, H^{c}), 7.65–7.67 (m, 3H, H$^{f'}$ + H$^{g'}$ + H$^{a''}$), 7.59 (d, $^3J_{H,H}$ = 9.2 Hz, 1H, H$^{e'}$), 7.55 (ddd, $^3J_{H,H}$ = 8.5 Hz, $^3J_{H,H}$ = 6.7 Hz, $^4J_{H,H}$ = 1.0 Hz, 1H, H$^{i''}$), 7.39–7.42 (m, 3H, H^{g} + H$^{i'}$ + H$^{h''}$), 7.35–7.37 (m, 2H, H^{d} + H^{f}), 7.19–7.22 (m, 2H, H^{e} + H$^{h'}$), 7.11–7.13 (m, 2H, H^{j} + H$^{e''}$), 7.08 (m, 2H, H^{a} + H^{b}), 6.87–6.89 (m, 1H, H^{h}), 6.53 (ddd, $^3J_{H,H}$ = 8.2 Hz, $^3J_{H,H}$ = 7.3 Hz, $^4J_{H,H}$ = 1.1 Hz, 1H, H^{i}), 5.31 (s, 1H, H$^{i'}$), 3.95 (s, 3H, CO$_2$CH'_3), 3.86 (s, 3H, CO$_2$CH''_3), 2.33 (s, 3H, Ar–CH_3), 2.01 (s, 3H, H^{α}), 1.11 ppm (s, 3H, H^{ε}); ^{13}C NMR (151 MHz, CDCl$_3$): δ = 189.3 (C^{β}), 187.3 (C^{δ}), 168.7 (C$^{9'}$), 167.3 (C^{9}), 166.6 (C$^{9''}$), 166.4 (C$''$O$_2$CH$_3$), 166.3 (C$'$O$_2$CH$_3$), 164.1 (C^{7}), 161.7 (C$^{7'}$), 156.6 (C$^{7''}$), 149.8 (C$^{2'}$), 146.5 (C^{2}), 145.6 (C$^{2''}$), 140.8 (C$^{1'}$), 138.6 (C$^{1''}$), 137.1 (C^{5}), 136.1 (C$^{11''}$), 135.7 (C^{3}), 135.4 (C^{11}), 135.3 (C$^{11'}$), 134.9 (C^{1}), 134.2 (C$^{17'}$), 133.6 (C^{17}), 133.07 (C^{4} or C^{6}), 133.04 (C$^{6''}$), 132.9 (C$^{17''}$), 132.1 (C^{4} or C^{6}), 131.0 (C$^{6'}$), 130.3 (C$^{4''}$), 130.0 (C$^{4'}$), 129.2 (C$^{13''}$), 128.9 (C$^{13'}$), 128.5 (C^{13}), 128.4 (C$^{5'}$), 128.0 (C$^{15''}$), 127.53 (C$^{12''}$), 127.51 (C$^{15'}$), 127.24 (C$^{5''}$), 127.17 (C^{15}), 126.5 (C$^{12'}$), 126.1 (C$^{10'}$), 125.9 (C^{12}), 124.6 (C^{10} + C$^{3'}$), 123.8 (C$^{14''}$), 122.3 (C$^{14'}$), 121.6 (C^{14}), 120.8 (C$^{10''}$), 119.8 (C$^{16''}$), 119.1 (C$^{16'}$), 118.3 (C^{16}), 117.6 (C$^{3''}$), 113.4 (C^{8}), 111.7 (C$^{8'}$), 109.5 (C$^{8''}$), 96.9 (C^{γ}), 52.4 (CO$_2$C$'$H$_3$), 52.1 (CO$_2$C$''$H$_3$), 26.5 (C^{α}), 25.2 (C^{ε}), 21.0 ppm (Ar–CH$_3$); ^{15}N{^{1}H} NMR (600 MHz, CDCl$_3$): δ = −125.6 (CH=N^3), −214.6 (CH=N^2–Co), −226.9 ppm (CH=N^1–Co); LRMS (ESI): *m/z* (%): 1046.245 (100) [*M* + Na]$^+$; HRMS (ESI): *m/z* calcd for C$_{61}$H$_{46}$CoN$_3$O$_9$ + Na: 1046.2458 [*M* + Na]$^+$; found: 1046.2451; elemental analysis calcd (%) for C$_{61}$H$_{46}$CoN$_3$O$_9$: C 71.55, H 4.53, N 4.10, Co 5.76; found: C 71.37, H 4.53, N 4.09, Co 5.73.

Crystals of **1d-Co(acac)** suitable for single-crystal X-ray diffraction analysis were obtained by vapor diffusion of MeCN into a solution of the complex in benzene. Crystal and refinement data are given in Table S6, SI.

1d-Lu. Ligand **1d** (0.219 g, 0.252 mmol, 1.0 equiv.) was dissolved in CH$_2$Cl$_2$ (5 mL). NEt$_3$ (0.30 mL, 2.2 mmol, 8.8 equiv.) was added, followed by a solution of Lu(NO$_3$)$_3$·xH$_2$O (0.117 g, 0.259 mmol, 1.0 equiv., assuming x = 5) in MeOH (10 mL). The reaction mixture was stirred at reflux temperature for 2 hours, and a yellow precipitate gradually formed. After cooling to rt, the precipitated solids were filtered off, washed with MeOH, and dried in an oven at 100 °C for 1 day, furnishing **1d-Lu** as a yellow solid. Yield: 0.216 g, 0.208 mmol, 82 %. ^{1}H NMR (600 MHz, [D$_6$]DMSO): δ = 8.68 (s, 2H, H$^{d'}$), 8.49 (s, 1H, H^{d}), 7.91 (d, $^3J_{H,H}$ = 8.6 Hz, 2H, H$^{j'}$), 7.77 (dd, $^3J_{H,H}$ = 7.9 Hz, $^4J_{H,H}$ = 1.6 Hz, 2H, H$^{b'}$), 7.68 (d, $^3J_{H,H}$ = 9.1 Hz, 1H, H^{f}), 7.61–7.64 (m, 4H, H$^{f'}$ + H$^{g'}$), 7.55 (d, $^3J_{H,H}$ = 7.3 Hz, 1H, H^{g}), 7.47 (d, $^3J_{H,H}$ = 8.7 Hz, 1H, H^{j}), 7.44 (d, $^3J_{H,H}$ = 7.9 Hz, 2H, H^{c}), 7.35–7.38 (m, 2H, H$^{i'}$), 7.29–7.32 (m, 4H, H^{a} + H$^{a'}$), 7.17–7.22 (m, 3H, H^{i} + H$^{h'}$), 7.05–7.08 (m, 1H, H^{h}), 6.77 (d, $^3J_{H,H}$ = 9.1 Hz, 1H, H^{e}), 6.05 (s (d expected), 2H, H$^{e'}$), 3.72 (s, 6H, CO$_2$CH_3), 2.37 ppm (s, 3H, Ar–CH_3); ^{13}C NMR (151 MHz, [D$_6$] DMSO): δ = 169.5 (C^{9}), 168.6 (C$^{9'}$), 165.5 (CO$_2$CH$_3$), 164.9 (C^{7}), 164.4 (C$^{7'}$), 153.5 (C$^{2'}$), 143.5 (C^{2}), 137.6 (C$^{1'}$), 136.4 (C^{11}), 136.1 (C^{4}), 135.6 (C$^{11'}$), 134.62 (C$^{17'}$), 134.61 (C^{17}), 133.1 (C^{1}), 131.0 (C$^{6'}$), 130.1 (C^{3}), 130.0 (C$^{4'}$), 128.7 (C^{13} + C$^{13'}$), 127.5 (C^{15}), 127.4 (C$^{15'}$), 126.1 (C$^{5'}$), 125.4 (C$^{12'}$), 125.3 (C^{12}), 125.0 (C^{10}), 124.5 (C$^{3'}$), 121.6 (C^{14} + C$^{14'}$), 119.6 (C$^{16'}$), 118.2 (C^{16}), 114.1 (C$^{8'}$), 110.3 (C^{8}), 52.2 (CO$_2$CH_3), 20.5 ppm (Ar–CH$_3$). Several of the ^{1}H and ^{13}C NMR resonances were broadened. The resonance corresponding to C$^{8'}$ could only be detected indirectly by HMBC experiments (600 MHz). The resonance corresponding to C$^{10'}$ was not observed at ambient temperature, but could be observed at 90 °C (δ 123.9; 125 MHz). ^{15}N{^{1}H} NMR (600 MHz, [D$_6$]DMSO): δ =

−112.2 (CH=N^2-Lu), −118.0 ppm (CH=N^1–Lu); LRMS (ESI): *m/z* (%): 890.284 (20) [**1d** + Na]$^+$, 1062.201 (100) [*M* + Na]$^+$; HRMS (ESI): *m/z* calcd for $C_{56}H_{38}LuN_3O_7$ + Na: 1062.2010 [*M* + Na]$^+$; found: 1062.2013; elemental analysis calcd (%) for $C_{56}H_{38}N_3O_7Lu$: C 64.68, H 3.68, N 4.04, Lu 16.83; found: C 63.59, H 3.92, N 4.16, Lu 16.49.

For additional NMR data for **1d-Lu** in different solvents and at different temperatures, see SI. For a discussion of the NMR characterization of **1d-Lu** in $CDCl_3$, see SI. **1d-Lu** was crystallographically characterized as **1d-Lu**–**DMSO** and **1d-Lu**–**MeOH**. Crystals of **1d-Lu**–**DMSO** suitable for single-crystal X-ray diffraction analysis were obtained by slow diffusion of EtOH into a solution of **1d-Lu** in DMSO. Crystal and refinement data are given in Table S12, SI. Crystals of **1d-Lu**–**MeOH** were obtained by slow diffusion of MeOH into a solution of **1d-Lu** in $CDCl_3$. Crystal and refinement data are given in Table S13, SI. A low carbon content was observed in the elemental analysis of **1d-Lu**. The low carbon content may be explained by the presence of one water ligand in the complex, although it is difficult to prove its presence unambiguously. For more info on potential water-ligation in **1d-Lu**, see SI.

Deposition Numbers 2021584 (for **8-Co(acac)**), 2021585 (for **9-Cu**), 2021586 (for **9-Ni**), 2021587 (for **2a-Zn**), 2021588 (for **1a-Zn**), 2021589 (for **3-Zn**–**MeOH**), 2021590 (for **1b-Zn**–NH_2), 2021591 (for **1b-Cd**–NH_2), 2054568 (for **1d-Zn**), 2054771 (for **1d-Co(acac)**), 2054854 (for **1b-Cu**–NH_2), 2053903 (for **1a-Cu**–NH_2), 2054825 (for **1d**), 2054856 (for **1d-Lu**–**DMSO**), and 2054826 (for **1d-Lu**–**MeOH**) contain the supplementary crystallographic data for this paper. These data are provided free of charge by the joint Cambridge Crystallographic Data Centre and Fachinformationszentrum Karlsruhe Access Structures service www.ccdc.cam.ac.uk/structures.

Acknowledgements

The Research Council of Norway is kindly acknowledged for funding through project no. 228157 (stipend to K.T.H). This work was also partly supported by the Research Council of Norway through the Norwegian NMR Package in 1994 and partly supported by the Research Council of Norway through the Norwegian NMR Platform, NNP (226244/F50). Additional support by the Department of Chemistry and the Faculty of Mathematics and Natural Sciences at University of Oslo is also acknowledged. We thank Principal Engineer Osamu Sekiguchi and Principal Engineer Lina Aarsbog, both University of Oslo, for performing the MS experiments. Furthermore, we thank Prof. Frode Rise and Senior Engineer Dirk Petersen, both University of Oslo, for providing generous access to the NMR facilities. We thank Dr. Richard H. Heyn (SINTEF Industry) for assistance with the elemental analyses. We acknowledge use of the Norwegian National Centre for X-ray Diffraction and Scattering (RECX).

Conflict of Interest

The authors declare no conflict of interest.

Keywords: Cadmium · Copper · Rare earth metals · Schiff base ligands · Zinc

[1] R. Hernández-Molina, A. Mederos, in *Comprehensive Coordination Chemistry II* (Eds.: J. A. McCleverty, T. J. Meyer), Pergamon, Oxford, **2003**, pp. 411–446.
[2] X. Liu, J.-R. Hamon, *Coord. Chem. Rev.* **2019**, *389*, 94–118.
[3] a) P. G. Cozzi, *Chem. Soc. Rev.* **2004**, *33*, 410–421; b) K. Matsumoto, B. Saito, T. Katsuki, *Chem. Commun.* **2007**, 3619–3627; c) X. Wu, C. Chen, Z. Guo, M. North, A. C. Whitwood, *ACS Catal.* **2019**, *9*, 1895–1906; d) X. Liu, C. Manzur, N. Novoa, S. Celedón, D. Carrillo, J.-R. Hamon, *Coord. Chem. Rev.* **2018**, *357*, 144–172.
[4] a) A. Erxleben, *Inorg. Chim. Acta* **2018**, *472*, 40–57; b) J. C. Pessoa, I. Correia, *Coord. Chem. Rev.* **2019**, *388*, 227–247; c) N. Kumar, Roopa, V. Bhalla, M. Kumar, *Coord. Chem. Rev.* **2021**, *427*, 213550; d) M. T. Kaczmarek, M. Zabiszak, M. Nowak, R. Jastrzab, *Coord. Chem. Rev.* **2018**, *370*, 42–54.
[5] a) A. W. Kleij, M. Kuil, D. M. Tooke, M. Lutz, A. L. Spek, J. N. H. Reek, *Chem. Eur. J.* **2005**, *11*, 4743–4750; b) S. H. A. M. Leenders, R. Gramage-Doria, B. de Bruin, J. N. H. Reek, *Chem. Soc. Rev.* **2015**, *44*, 433–448; c) A. W. Kleij, *Dalton Trans.* **2009**, 4635–4639.
[6] a) C. Freire, M. Nunes, C. Pereira, D. M. Fernandes, A. F. Peixoto, M. Rocha, *Coord. Chem. Rev.* **2019**, *394*, 104–134; b) J. L. Segura, M. J. Mancheño, F. Zamora, *Chem. Soc. Rev.* **2016**, *45*, 5635–5671; c) J. Zhang, L. Xu, W.-Y. Wong, *Coord. Chem. Rev.* **2018**, *355*, 180–198.
[7] C.-M. Che, J.-S. Huang, *Coord. Chem. Rev.* **2003**, *242*, 97–113.
[8] a) P. A. Vigato, S. Tamburini, *Coord. Chem. Rev.* **2004**, *248*, 1717–2128; b) S. Yamada, *Coord. Chem. Rev.* **1999**, *190–192*, 537–555; c) W. Radecka-Paryzek, V. Patroniak, J. Lisowski, *Coord. Chem. Rev.* **2005**, *249*, 2156–2175; d) P. A. Vigato, V. Peruzzo, S. Tamburini, *Coord. Chem. Rev.* **2012**, *256*, 953–1114.
[9] a) K. Bernardo, S. Leppard, A. Robert, G. Commenges, F. Dahan, B. Meunier, *Inorg. Chem.* **1996**, *35*, 387–396; b) A. Mrutu, A. C. Lane, J. M. Drewett, S. D. Yourstone, C. L. Barnes, C. M. Halsey, J. W. Cooley, J. R. Walensky, *Polyhedron* **2013**, *54*, 300–308; c) J. Rich, M. Rodríguez, I. Romero, X. Fontrodona, P. W. N. M. van Leeuwen, Z. Freixa, X. Sala, A. Poater, M. Solà, *Eur. J. Inorg. Chem.* **2013**, 1213–1224.
[10] a) A. Sahraei, H. Kargar, M. Hakimi, M. N. Tahir, *J. Mol. Struct.* **2017**, *1149*, 576–584; b) P. D. Frischmann, M. J. MacLachlan, *Chem. Commun.* **2007**, 4480–4482; c) J. Parr, A. T. Ross, A. M. Z. Slawin, *J. Chem. Soc. Dalton Trans.* **1996**, 1509–1512; d) J. Hamblin, L. J. Childs, N. W. Alcock, M. J. Hannon, *J. Chem. Soc. Dalton Trans.* **2002**, 164–169; e) E. C. Alyea, A. Malek, A. E. Vougioukas, *Can. J. Chem.* **1982**, *60*, 667–672; f) D. J. Berg, S. J. Rettig, C. Orvig, *J. Am. Chem. Soc.* **1991**, *113*, 2528–2532; g) J. K. Molloy, C. Philouze, L. Fedele, D. Imbert, O. Jarjayes, F. Thomas, *Dalton Trans.* **2018**, *47*, 10742–10751; h) E. E. Hardy, K. M. Wyss, R. J. Keller, J. D. Gorden, A. E. V. Gorden, *Dalton Trans.* **2018**, *47*, 1337–1346; i) W.-K. Wong, H. Liang, J. Guo, W.-Y. Wong, W.-K. Lo, K.-F. Li, K.-W. Cheah, Z. Zhou, W.-T. Wong, *Eur. J. Inorg. Chem.* **2004**, 829–836; j) D. Lionetti, V. W. Day, J. D. Blakemore, *Dalton Trans.* **2017**, *46*, 11779–11789; k) B. E. Klamm, C. J. Windorff, C. Celis-Barros, M. L. Marsh, D. S. Meeker, T. E. Albrecht-Schmitt, *Inorg. Chem.* **2018**, *57*, 15389–15398; l) S. T. Tsantis, A. Lagou-Rekka, K. F. Konidaris, C. P. Raptopoulou, V. Bekiari, V. Psycharis, S. P. Perlepes, *Dalton Trans.* **2019**, *48*, 15668–15678; m) B. E. Klamm, C. J. Windorff, M. L. Marsh, D. S. Meeker, T. E. Albrecht-Schmitt, *Chem. Commun.* **2018**, *54*, 8634–8636; n) B. E. Klamm, C. J. Windorff, C. Celis-Barros, M. J. Beltran-Leiva, J. M. Sperling, T. E. Albrecht-Schönzart, *Inorg. Chem.* **2020**, *59*, 18035–18047; o) T. Radoske, R. Kloditz, S. Fichter, J. März, P. Kaden, M. Patzschke, M. Schmidt, T. Stumpf, O. Walter, A. Ikeda-Ohno, *Dalton Trans.* **2020**, *49*, 17559–17570; p) T. Radoske, J. März, M. Patzschke, P. Kaden, O. Walter, M. Schmidt, T. Stumpf, *Chem. Eur. J.* **2020**, *26*, 16853–16859; q) F. Gao, F.-L. Yang, G.-Z. Zhu, Y. Zhao, *Dalton Trans.* **2015**, *44*, 20232–20241; r) H.-H. Chen, D.-F. Wu, Y.-Y. Duan, L. Li, Y.-J. Wang, X.-M. Zhang, J.-Z. Cui, H.-L. Gao, *New J. Chem.* **2020**, *44*, 2561–2570; s) E. E. Hardy, K. M. Wyss, J. D. Gorden, I. R. Ariyarathna, E. Miliordos, A. E. V. Gorden, *Chem. Commun.* **2017**, *53*, 11984–11987.
[11] a) M. Niemeyer, P. P. Power, *Inorg. Chem.* **1996**, *35*, 7264–7272; b) J. A. C. Clyburne, N. McMullen, *Coord. Chem. Rev.* **2000**, *210*, 73–99; c) M. Olaru, J. Beckmann, C. I. Raț, *Organometallics* **2014**, *33*, 3012–3020; d) M. A. Boreen, B. F. Parker, S. Hohloch, B. A. Skeel, J. Arnold, *Dalton Trans.* **2018**, *47*, 96–104; e) T. Wiedemann, G. Voit, A. Tchernook, P. Roesle, I. Göttker-Schnetmann, S. Mecking, *J. Am. Chem. Soc.* **2014**, *136*, 2078–2085; f) R. C. Smith, J. D. Protasiewicz, *Organometallics* **2004**, *23*, 4215–4222; g) R. C. Smith, C. R. Bodner, M. J. Earl, N. C. Sears, N. E. Hill, L. M. Bishop, N. Sizemore, D. T. Hehemann, J. J. Bohn, J. D. Protasiewicz, *J. Organomet. Chem.* **2005**, *690*, 477–481; h) B. R. Barnett, C. C. Mokhtarzadeh, J. S. Figueroa, P. Lummis, S. Wang, J. Gavenonis, N. Schüwer, T. D. Tilley, J. N. Boynton, P. P. Power, T. B. Ditri, N. Weidemann, D. W. Agnew,

P. W. Smith, A. E. Carpenter, J. K. Pratt, N. D. Mendelson, J. D. Queen, in *Inorganic Syntheses* (Ed.: P. P. Power), **2018**, pp. 85–122; i) A. S. Crossman, A. T. Larson, J. X. Shi, S. M. Krajewski, E. S. Akturk, M. P. Marshak, *J. Org. Chem.* **2019**, *84*, 7434–7442; j) E. J. Hopkins, S. M. Krajewski, A. S. Crossman, F. D. R. Maharaj, L. T. Schwanz, M. P. Marshak, *Eur. J. Inorg. Chem.* **2020**, 1951–1959.

[12] C. Wei, Y. He, X. Shi, Z. Song, *Coord. Chem. Rev.* **2019**, *385*, 1–19.

[13] a) A. Kayal, A. F. Ducruet, S. C. Lee, *Inorg. Chem.* **2000**, *39*, 3696–3704; b) G. A. Edouard, P. Kelley, D. E. Herbert, T. Agapie, *Organometallics* **2015**, *34*, 5254–5277.

[14] K. T. Hylland, S. Øien-Ødegaard, R. H. Heyn, M. Tilset, *Eur. J. Inorg. Chem.* **2020**, 3627–3643.

[15] a) X.-B. Lu, W.-M. Ren, G.-P. Wu, *Acc. Chem. Res.* **2012**, *45*, 1721–1735; b) M. H. Rønne, D. Cho, M. R. Madsen, J. B. Jakobsen, S. Eom, É. Escoudé, H. C. D. Hammershøj, D. U. Nielsen, S. U. Pedersen, M.-H. Baik, T. Skrydstrup, K. Daasbjerg, *J. Am. Chem. Soc.* **2020**, *142*, 4265–4275; c) M. R. Madsen, J. B. Jakobsen, M. H. Rønne, H. Liang, H. C. D. Hammershøj, P. Nørby, S. U. Pedersen, T. Skrydstrup, K. Daasbjerg, *Organometallics* **2020**, *39*, 1480–1490.

[16] a) M. Marcos, A. Omenat, J. Barberá, F. Durán, J. L. Serrano, *J. Mater. Chem.* **2004**, *14*, 3321–3327; b) C. J. Whiteoak, G. Salassa, A. W. Kleij, *Chem. Soc. Rev.* **2012**, *41*, 622–631; c) Y. Sunatsuki, Y. Motoda, N. Matsumoto, *Coord. Chem. Rev.* **2002**, *226*, 199–209.

[17] K. T. Hylland, S. Øien-Ødegaard, M. Tilset, *Eur. J. Org. Chem.* **2020**, 4208–4226.

[18] a) D. X. Hu, P. Grice, S. V. Ley, *J. Org. Chem.* **2012**, *77*, 5198–5202; b) R. A. Al-Horani, U. R. Desai, *Tetrahedron* **2012**, *68*, 2027–2040.

[19] A. Bruylants, E. F.-D. Medicis, in *Carbon-Nitrogen Double Bonds (1970)* (Ed.: S. Patai), John Wiley & Sons Ltd., Great Britain, **1970**, pp. 465–504.

[20] G. Consiglio, S. Failla, P. Finocchiaro, I. P. Oliveri, S. D. Bella, *Dalton Trans.* **2012**, *41*, 387–395.

[21] a) S. J. Wezenberg, G. A. Metselaar, E. C. Escudero-Adán, J. Benet-Buchholz, A. W. Kleij, *Inorg. Chim. Acta* **2009**, *362*, 1053–1057; b) F. Castro-Gómez, G. Salassa, A. W. Kleij, C. Bo, *Chem. Eur. J.* **2013**, *19*, 6289–6298; c) W. Lamine, S. Boughdiri, L. Christ, C. Morell, H. Chermette, *J. Comput. Chem.* **2019**, *40*, 717–725.

[22] a) O. Schlager, K. Wieghardt, H. Grondey, A. Rufinska, B. Nuber, *Inorg. Chem.* **1995**, *34*, 6440–6448; b) A. Sokolowski, J. Müller, T. Weyhermüller, R. Schnepf, P. Hildebrandt, K. Hildenbrand, E. Bothe, K. Wieghardt, *J. Am. Chem. Soc.* **1997**, *119*, 8889–8900; c) K. P. Wainwright, *Coord. Chem. Rev.* **1997**, *166*, 35–90.

[23] a) B. Samanta, J. Chakraborty, S. Shit, S. R. Batten, P. Jensen, J. D. Masuda, S. Mitra, *Inorg. Chim. Acta* **2007**, *360*, 2471–2484; b) S. Basak, S. Sen, S. Banerjee, S. Mitra, G. Rosair, M. T. G. Rodriguez, *Polyhedron* **2007**, *26*, 5104–5112; c) M. Orio, C. Philouze, O. Jarjayes, F. Neese, F. Thomas, *Inorg. Chem.* **2010**, *49*, 646–658; d) G. Consiglio, S. Failla, P. Finocchiaro, I. P. Oliveri, S. Di Bella, *Inorg. Chem.* **2012**, *51*, 8409–8418.

[24] a) G. Forte, I. P. Oliveri, G. Consiglio, S. Failla, S. Di Bella, *Dalton Trans.* **2017**, *46*, 4571–4581; b) G. Consiglio, I. P. Oliveri, S. Failla, S. Di Bella, *Molecules* **2019**, *24*, 2514.

[25] a) E. W. Abel, N. J. Long, K. G. Orrell, A. G. Osborne, H. M. Pain, V. Šik, *J. Chem. Soc. Chem. Commun.* **1992**, 303–304; b) E. R. Civitello, P. S. Dragovich, T. B. Karpishin, S. G. Novick, G. Bierach, J. F. O'Connell, T. D. Westmoreland, *Inorg. Chem.* **1993**, *32*, 237–241.

[26] a) K. G. Orrell, in *Annu. Rep. NMR Spectrosc., Vol. 37* (Ed.: G. A. Webb), Academic Press, **1999**, pp. 1–74; b) K. G. Orrell, A. G. Osborne, J. O. Prince, V. Šik, D. K. Vellianitis, *Eur. J. Inorg. Chem.* **2000**, 383–391; c) M. L. Creber, K. G. Orrell, A. G. Osborne, V. Šik, M. B. Hursthouse, M. E. Light, *Polyhedron* **2001**, *20*, 1973–1982.

[27] a) L. Pazderski, *Magn. Reson. Chem.* **2008**, *46*, S3-S15; b) R. Kleinmaier, S. Arenz, A. Karim, A.-C. C. Carlsson, M. Erdélyi, *Magn. Reson. Chem.* **2013**, *51*, 46–53; c) J. Jaźwiński, *J. Mol. Struct.* **2005**, *750*, 7–17; d) D. Niedzielska, T. Pawlak, A. Wojtczak, L. Pazderski, E. Szlyk, *Polyhedron* **2015**, *92*, 41–51.

[28] A. W. Addison, T. N. Rao, J. Reedijk, J. van Rijn, G. C. Verschoor, *J. Chem. Soc. Dalton Trans.* **1984**, 1349–1356.

[29] J. A. Connor, M. Charlton, D. C. Cupertino, A. Lienke, M. McPartlin, I. J. Scowen, P. A. Tasker, *J. Chem. Soc. Dalton Trans.* **1996**, 2835–2838.

[30] A. W. Kleij, M. Kuil, M. Lutz, D. M. Tooke, A. L. Spek, P. C. J. Kamer, P. W. N. M. van Leeuwen, J. N. H. Reek, *Inorg. Chim. Acta* **2006**, *359*, 1807–1814.

[31] a) A. Okuniewski, D. Rosiak, J. Chojnacki, B. Becker, *Polyhedron* **2015**, *90*, 47–57; b) D. Rosiak, A. Okuniewski, J. Chojnacki, *Polyhedron* **2018**, *146*, 35–41.

[32] E. C. Constable, G. Zhang, C. E. Housecroft, M. Neuburger, J. A. Zampese, *Inorg. Chim. Acta* **2010**, *363*, 4207–4213.

[33] M. Shi, W.-L. Duan, *Appl. Organomet. Chem.* **2003**, *17*, 175–180.

[34] a) S. G. Telfer, T. Sato, T. Harada, R. Kuroda, J. Lefebvre, D. B. Leznoff, *Inorg. Chem.* **2004**, *43*, 6168–6176; b) J.-M. Xiao, W. Zhang, *Inorg. Chem. Commun.* **2009**, *12*, 1175–1178; c) P. Liu, X.-J. Feng, R. He, *Tetrahedron* **2010**, *66*, 631–636.

[35] D. DiMondo, M. E. Thibault, J. Britten, M. Schlaf, *Organometallics* **2013**, *32*, 6541–6554.

[36] a) D. F. Evans, *J. Chem. Soc.* **1959**, 2003–2005; b) K. De Buysser, G. G. Herman, E. Bruneel, S. Hoste, I. Van Driessche, *Chem. Phys.* **2005**, *315*, 286–292.

[37] A. B. P. Lever, *Inorg. Chem.* **1965**, *4*, 763–764.

[38] a) S. Mariko, S. Hisako, M. Yukie, F. Yutaka, *Bull. Chem. Soc. Jpn.* **2009**, *82*, 1266–1273; b) S. Mukhopadhyay, D. Mandal, D. Ghosh, I. Goldberg, M. Chaudhury, *Inorg. Chem.* **2003**, *42*, 8439–8445.

[39] T. P. Cheeseman, D. Hall, T. N. Waters, *J. Chem. Soc. A* **1966**, 1396–1406.

[40] a) J. B. Jakobsen, M. H. Rønne, K. Daasbjerg, T. Skrydstrup, *Angew. Chem. Int. Ed.* **2021**, *60*, 9174–9179; b) N. W. Kinzel, C. Werlé, W. Leitner, *Angew. Chem. Int. Ed.*, DOI: doi.org/10.1002/anie.202006988.

[41] a) M. Franks, A. Gadzhieva, L. Ghandhi, D. Murrell, A. J. Blake, E. S. Davies, W. Lewis, F. Moro, J. McMaster, M. Schröder, *Inorg. Chem.* **2013**, *52*, 660–670; b) A. K. Nairn, S. J. Archibald, R. Bhalla, B. C. Gilbert, E. J. MacLean, S. J. Teat, P. H. Walton, *Dalton Trans.* **2006**, 172–176; c) E. Bill, J. Müller, T. Weyhermüller, K. Wieghardt, *Inorg. Chem.* **1999**, *38*, 5795–5802; d) F. Thomas, O. Jarjayes, C. Duboc, C. Philouze, E. Saint-Aman, J.-L. Pierre, *Dalton Trans.* **2004**, 2662–2669.

[42] S. Zolezzi, A. Decinti, E. Spodine, *Polyhedron* **1999**, *18*, 897–904.

[43] a) M. K. Paira, J. Dinda, T. H. Lu, A. R. Paital, C. Sinha, *Polyhedron* **2007**, *26*, 4131–4140; b) V. Lozovan, V. Ch Kravtsov, E. B. Coropceanu, P. Rotaru, A. V. Siminel, M. S. Fonari, *Inorg. Chim. Acta* **2019**, *491*, 42–51; c) M. Martínez Belmonte, E. C. Escudero-Adán, E. Martin, A. W. Kleij, *Dalton Trans.* **2012**, *41*, 5193–5200.

[44] a) W.-K. Lo, W.-K. Wong, W.-Y. Wong, J. Guo, *Eur. J. Inorg. Chem.* **2005**, 3950–3954; b) P. D. Frischmann, G. A. Facey, P. Y. Ghi, A. J. Gallant, D. L. Bryce, F. Lelj, M. J. MacLachlan, *J. Am. Chem. Soc.* **2010**, *132*, 3893–3908.

[45] Q. Shi, L. Xu, J. Ji, Y. Li, R. Wang, Z. Zhou, R. Cao, M. Hong, A. S. C. Chan, *Inorg. Chem. Commun.* **2004**, *7*, 1254–1257.

[46] a) D. Reinen, C. Friebel, *Inorg. Chem.* **1984**, *23*, 791–798; b) I. B. Bersuker, *Chem. Rev.* **2001**, *101*, 1067–1114.

[47] a) N. Charef, F. Sebti, L. Arrar, M. Djarmouni, N. Boussoualim, A. Baghiani, S. Khennouf, A. Ourari, M. A. AlDamen, M. S. Mubarak, D. G. Peters, *Polyhedron* **2015**, *85*, 450–456; b) M. A. AlDamen, N. Charef, H. K. Juwhari, K. Sweidan, M. S. Mubarak, D. G. Peters, *J. Chem. Crystallogr.* **2016**, *46*, 411–420.

[48] a) M. A. Halcrow, *Chem. Soc. Rev.* **2013**, *42*, 1784–1795; b) B. Murphy, B. Hathaway, *Coord. Chem. Rev.* **2003**, *243*, 237–262.

[49] R. Shannon, *Acta Crystallogr. Sect. A* **1976**, *32*, 751–767.

[50] J.-C. G. Bünzli, *J. Coord. Chem.* **2014**, *67*, 3706–3733.

[51] Orvig and co-workers reported that the reactions between potentially heptadentate Schiff base ligands (H_3L) and $Ln(NO_3)_3 \cdot xH_2O$ yielded nonacoordinated $Ln(H_3L)(NO_3)_3$ complexes where the ligands in fact acted as neutral tridentate O_3 ligands, rather than heptadentate $N_4O_3^{3-}$ ligands. By using the corresponding chloride salts they obtained complexes of the type Ln(L) with the ligands being heptadentate. A. Smith, S. J. Rettig, C. Orvig, *Inorg. Chem.* **1988**, *27*, 3929–3934.

[52] a) Y. Yao, H.-Y. Yin, Y. Ning, J. Wang, Y.-S. Meng, X. Huang, W. Zhang, L. Kang, J.-L. Zhang, *Inorg. Chem.* **2019**, *58*, 1806–1814; b) K. Masatoshi, Y. Toshiro, *Chem. Lett.* **1999**, *28*, 137–138.

[53] a) J. Harrowfield, M. Ogden, A. White, *Aust. J. Chem.* **1991**, *44*, 1237–1247; b) L. Semenova, B. Skelton, A. White, *Aust. J. Chem.* **1996**, *49*, 997–1004; c) A. Abbasi, E. Damian Risberg, L. Eriksson, J. Mink, I. Persson, M. Sandström, Y. V. Sidorov, M. Y. Skripkin, A.-S. Ullström, *Inorg. Chem.* **2007**, *46*, 7731–7741; d) Z. Asfari, E. J. Chan, J. M. Harrowfield, B. W. Skelton, A. N. Sobolev, P. Thuéry, A. H. White, *Aust. J. Chem.* **2020**, *73*, 447–454; e) M. E. Minyaev, I. E. Nifant'ev, A. N. Tavtorkin, S. y A. Korchagina, S. S. Zeynalova, I. V. Ananyev, A. V. Churakov, *Acta Crystallogr. Sect. C* **2017**, *73*, 820–827; f) J.-i. Setsune, K. Watanabe, *J. Porphyrins Phthalocyanines* **2012**, *16*, 508–517.

[54] L. G. Nielsen, A. K. R. Junker, T. J. Sørensen, *Dalton Trans.* **2018**, *47*, 10360–10376.

[55] W. Zhou, D. McKearney, D. B. Leznoff, *Chem. Eur. J.* **2020**, *26*, 1027–1031.

[56] a) J. P. Jesson, E. L. Muetterties, in *Dynamic Nuclear Magnetic Resonance Spectroscopy* (Eds.: L. M. Jackman, F. A. Cotton), Academic Press, **1975**, pp. 253–316; b) U. Casellato, S. Tamburini, P. Tomasin, P. A. Vigato, S.

Aime, M. Botta, *Inorg. Chem.* **1999**, *38*, 2906–2916; c) V. Peruzzo, A. Lanza, F. Nestola, P. A. Vigato, S. Tamburini, *Inorg. Chim. Acta* **2014**, *416*, 226–234; d) J. Kotek, V. Kubíček, P. Hermann, I. Lukeš, in *The Chemistry of Contrast Agents in Medical Magnetic Resonance Imaging*, 2nd. ed. (Eds.: A. Merbach, L. Helm, É. Tóth), John Wiley & Sons, Ltd, Great Britain, **2013**, pp. 83–155; e) J.-P. Costes, A. Dupuis, G. Commenges, S. Lagrave, J.-P. Laurent, *Inorg. Chim. Acta* **1999**, *285*, 49–54.

[57] For additional NMR studies of **1d-Lu** in a non-donating solvent ($CDCl_3$), see SI.

[58] B. L. Ramirez, P. Sharma, R. J. Eisenhart, L. Gagliardi, C. C. Lu, *Chem. Sci.* **2019**, *10*, 3375–3384.

[59] For examples of Schiff base complexes of rare earth metals as polymerization catalysts: a) C. Bakewell, T.-P.-A. Cao, N. Long, X. F. Le Goff, A. Auffrant, C. K. Williams, *J. Am. Chem. Soc.* **2012**, *134*, 20577–20580; b) A. Decortes, R. M. Haak, C. Martín, M. M. Belmonte, E. Martin, J. Benet-Buchholz, A. W. Kleij, *Macromolecules* **2015**, *48*, 8197–8207; c) W. Gu, P. Xu, Y. Wang, Y. Yao, D. Yuan, Q. Shen, *Organometallics* **2015**, *34*, 2907–2916; d) C.-H. Ho, H.-J. Chuang, P.-H. Lin, B.-T. Ko, *J. Polym. Sci. Part A* **2017**, *55*, 321–328; e) R. Xu, L. Hua, X. Li, Y. Yao, X. Leng, Y. Chen, *Dalton Trans.* **2019**, *48*, 10565–10573.

[60] S. Tanase, S. Sottini, V. Marvaud, E. J. J. Groenen, L.-M. Chamoreau, *Eur. J. Inorg. Chem.* **2010**, 3478–3483.

[61] L.-W. Yang, S. Liu, E. Wong, S. J. Rettig, C. Orvig, *Inorg. Chem.* **1995**, *34*, 2164–2178.

[62] a) C.-P. Wong, G. Bisset, in *Inorganic Syntheses* (Ed.: S. L. Holt Jr.), **1984**, pp. 156–162; b) W. Xie, M. J. Heeg, P. G. Wang, *Inorg. Chem.* **1999**, *38*, 2541–2543; c) H. He, W.-K. Wong, J. Guo, K.-F. Li, W.-Y. Wong, W.-K. Lo, K.-W. Cheah, *Inorg. Chim. Acta* **2004**, *357*, 4379–4388; d) S. Tamburini, S. Sitran, V. Peruzzo, P. A. Vigato, *Eur. J. Inorg. Chem.* **2009**, 155–167.

[63] For examples of the utilization of $Ln[N(TMS)_2]_3$ as starting materials for the synthesis of Ln Schiff base complexes: a) S. A. Schuetz, V. W. Day, R. D. Sommer, A. L. Rheingold, J. A. Belot, *Inorg. Chem.* **2001**, *40*, 5292–5295; b) S. A. Schuetz, C. M. Silvernail, C. D. Incarvito, A. L. Rheingold, J. L. Clark, V. W. Day, J. A. Belot, *Inorg. Chem.* **2004**, *43*, 6203–6214; c) F. Han, Q. Teng, Y. Zhang, Y. Wang, Q. Shen, *Inorg. Chem.* **2011**, *50*, 2634–2643; d) W. Lv, Y. Wang, B. Wu, Y. Yao, Q. Shen, *Z. Anorg. Allg. Chem.* **2012**, *638*, 1167–1172; e) W. Ren, L. Chen, N. Zhao, Q. Wang, G. Hou, G. Zi, *J. Organomet. Chem.* **2014**, *758*, 65–72.

[64] G. M. Sheldrick, *Acta Crystallogr. Sect. A* **2015**, *71*, 3–8.

[65] G. M. Sheldrick, *Acta Crystallogr. Sect. C* **2015**, *71*, 3–8.

[66] O. V. Dolomanov, L. J. Bourhis, R. J. Gildea, J. A. K. Howard, H. Puschmann, *J. Appl. Crystallogr.* **2009**, *42*, 339–341.

[67] F. H. Allen, O. Johnson, G. P. Shields, B. R. Smith, M. Towler, *J. Appl. Crystallogr.* **2004**, *37*, 335–338.

[68] A. Spek, *Acta Crystallogr. Sect. C* **2015**, *71*, 9–18.

Manuscript received: February 25, 2021
Revised manuscript received: March 24, 2021
Accepted manuscript online: March 26, 2021